University of South-Eastern Norway
Faculty of Technology, Natural Sciences and Maritime Sciences

–

Master's Thesis

Study programme: Master of Science in Micro and Nano Systems Technology

Spring/Autumn 2023

Javeria Shabbir

Optimized Microstructure Al Substrate for iCL-CNT Growth for High Energy Density Supercapacitors

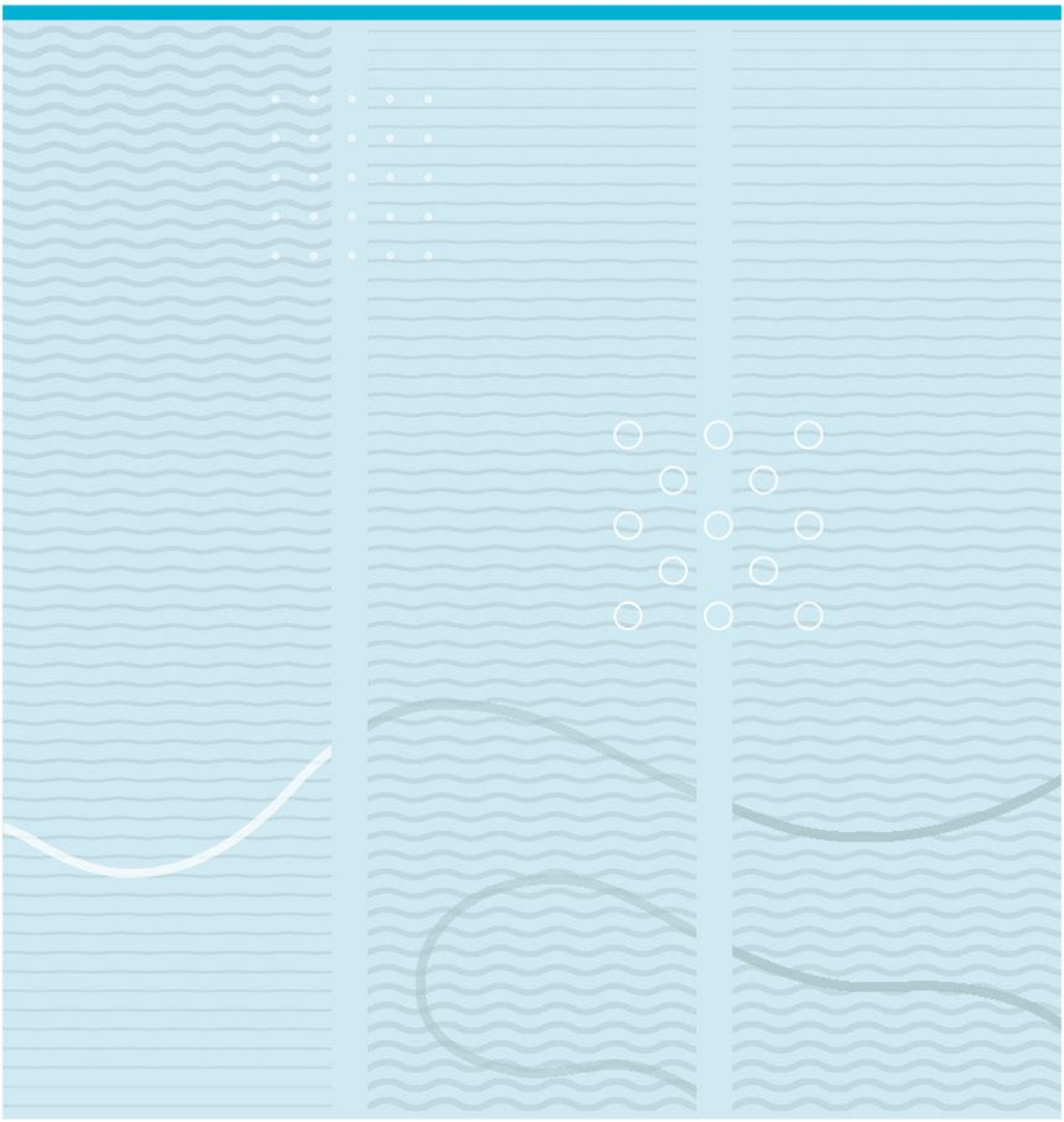

University of South-Eastern Norway
Faculty of Technology, Natural Sciences and Maritime Sciences
Department of Microsystems.
Raveien 215
NO-3184 Borre, Norway

http://www.usn.no

Summary

The thesis study investigates the effect of Al surface morphology on the growth of inter-connected cross-linked carbon nanotubes for high-energy-density supercapacitors. This study aims to improve the electrochemical performance of supercapacitors by modifying the morphology of Al substrate to increase the surface area.

The study proposes a low-cost yet highly efficient chemical etching technique to modify pristine Al to introduce microstructures on the surface. It explores the impact of time, and temperature on the etched morphology of two different thicknesses of foils (Al-15p, Al-30p). A comparison is made between the samples, by measuring surface roughness using AFM. Furthermore, a systematic study is made by comparing the Ni deposition and CNTs growth on chemically etched foils with the commercially purchased anodic etched Al foils, to evaluate the difference in electrochemical performance based on different etching methods.

The increase in surface area and its effect after CNTs growth is confirmed by the preparation of electrodes using pristine, chemically etched, and commercially anodic etched foils by evaluating the Cyclic Voltammetry curve of electrodes using a 3-electrode setup in an aqueous Na_2SO_4 electrolyte. The resultant capacitance reveals the chemically etched samples exhibited an increase in surface area by ~1.8 times compared to pristine samples. The etching also proves the better adhesion of CNTs to the modified substrate as compared to the smooth substrate.

Overall, the electrochemical results achieved from the CNTs-grown on chemically etched samples accomplished the capacitance of approximately (Al-15CE:26.50mF/cm^2, Al-30CE:24.0mF/cm^2), which is comparable to the capacitance of CNTs electrodes made from commercially purchased anodic etched foil (Al-70: 21.0 mF/cm^2, Al-30: 21.20 mF/cm^2).

Acknowledgment

I am truly thankful for the invaluable assistance and support I received throughout this master project from the enormous group of individuals. First and foremost, I would like to express my sincere gratitude to the University of South-eastern Norway for allowing me to pursue this master's degree.

I extend my heartfelt appreciation to my supervisor Dr. Xuyuan Chen his unwavering guidance steered me in the right direction. I am also thankful to nanoCaps AS and Per Ohlckers for granting me the opportunity to work on their ongoing research project, and for assigning Dr. Raghunandan Ummethala as my co-supervisor. My supervisor's whole-heartedness support, motivation, and guidance have been instrumental in helping me to achieve my results. Here I would also like to Thank Pai-Lu for his help and guidance.

Special Thanks to deliberate lab engineers Zekija Ramic for helping me in my Lab sessions and Gaurav Sharma for always helping me without any reluctance.

Lastly, I would like to express my gratitude to my friends and especially my family for their support and motivation during my academic pursuit.

Contents

List of Figures

List of Tables

1 Introduction

With the passage of time mankind need for energy sources is increasing with the increasing population and has become the main concern for all world leading economies. Mainly the technological evolution of energy generation, storage, and conversion plays a vital role in fulfilling the energy demand. But with the limitation of energy generation methods like nuclear plants, it is difficult to achieve the world's needs. Therefore, one of the environment-friendly solutions is to use renewable energy sources such as solar, and wind which are increasingly being used [1]. The only drawback with these energy sources is the absence of external factors which they depend on like the presence of sun and wind, which further leads to the usage of modern energy storage technologies to store energy.

In the energy storage context, the most recent advances have been made in the sector of Li-ion storage batteries because of their characteristics like longer cycle life, and discharge properties [2]. Li-ion batteries lack high power density, limiting their usage in integrated modules. Therefore, with the development in the electric industry, Supercapacitors have gained extensive fame for their high power and energy density, fast charge/discharge properties, and long life span, and becoming a hot research topic in the field of energy storage for the next generations [3].

Various types of supercapacitors can give various properties, Electric double layer Supercapacitors are best suited for high power density while Pseudo-capacitors can be used to get high energy density. This study proceeds with Electric Double Layer Capacitors (EDLCs), which are energy storage devices with the characteristics like high power density, low internal resistance, wide thermal range (-40°C - 70°C), and longer life span. The inner mechanism of the supercapacitor that is based on the charge separation at the interface of electrode and electrolyte makes it capable to deliver the charge at a relatively higher rate as compared to batteries[4].

A supercapacitor consists of current collectors, electrodes, separators, and an electrolyte. To increase the efficiency of supercapacitors studies have been made on the material of electrodes which plays a vital role to increase the capacitance of supercapacitors. Few achievements have been made by using various materials of electrodes like activated carbon [5], Graphene [6], Carbon nanotubes [7], and Silicon oxide [8]. To support the electrodes, current collector is an essential part of supercapacitors as together with electrode current collectors carries 15 to 20% of the total weight of the

supercapacitor, thus it have a great influence on the performance of Supercapacitor [9]. Since, the electrodes are responsible for storing the charge and current collectors transfer the charge while the charging/discharging process**.** The factors like surface area and, the electrical conductivity of current collector and electrode have great impact on the electrochemical performance of the Supercapacitor's electrode material. Therefore, in recent studies electrodes and current collectors are downsized to the nanoscale to enhance the SC's performance. Exclusively, the nanostructured current collectors provide the growth of nanostructured electrodes and also offer the enhanced and conductive surface area for charge transportation. This brings the need for comprehensive optimization and study on current collector to enhance the surface area and electrical conductivity of the electrode [10].

Previous research studies have revealed that the smooth metallic current collectors with carbon layer often peels off after running certain cycles of charge/discharge that further results in poor electrochemical performance of SCs. Various research studies have been conducted to overcome this peeling effect. Recently manufacturers have started using the nanostructured substrate by using different techniques surface lasering effect, sol-gel deposition, plasma enhancement, Electrochemical etching, etc [11]. Some of the studies show the effect on the electrochemical properties of SCs by using nanostructured Ni mesh and foams as a current collectors [12]. [13] reveals the better electrochemical performance of current collectors which are facile coated by graphene and carbon black graphene for iron phosphate lithium-ion batteries. The proposed study in this research investigates the cost-effective chemical etching method as an alternative to above mentioned expensive procedures with less complexity.

1.1 Research Motivation

The motivation for this thesis is to improve the energy density of supercapacitors by optimizing the microstructure Al substrate. Since the energy density of SC is directly proportional to specific capacitance and square of voltage range, according to eq 1.1 [14].

$$E = \frac{1}{2}CV^2 \qquad 1.1$$

$$C = \frac{\varepsilon A}{d} \qquad 1.2$$

Capacitance depends on the area of electrodes and *d* is the distance between electrodes. In the present work, the low-cost, easy to clean, and sustainable solution is proposed to fabricate high-performance Al current collector for the application of Supercapacitors. Which further improves the properties like; better adhesion between electrode and current collector, and increases the surface area, mechanical strength. Therefore, by improving the specific capacitance of electrode the energy density can be improved.

1.2 Research Approaches

Therefore, to address the need, this study has been made on the optimization of Al foil by etching the Pristine Al foil of two different thicknesses. This research study has adopted the chemical Etching technique, where the etching of Al foil is performed by changing the parameters like time and temperature of etching with the commercially purchased etchant composite of phosphoric(H_3PO_4) , nitric(HNO_3), acetic acid(CH_3COOH), and water (H_2O). To the best of our knowledge, no previous studies have been conducted using this composite etchant.

Proceeds with the SEM analysis to see the temperature and time impact on morphology, and a comparative morphology study is made for chemically etched Al foil. Furthermore, SEM analysis on commercially purchased etched foil is made to analyze the difference between chemically etched morphology with the commercially anodic etched Morphology. To quantify the differences in roughness parameters of etched samples, AFM is used to compare the average surface roughness with pristine foils. Further, the Ni particle is deposited on pristine, chemically, and commercially etched samples by using the Sputtering method, which is followed by the SEM analysis of Ni morphology. Afterward, CVD is performed to grow CNTs on all these substrates.

A complete systematic study is made by using SEM and electrochemically testing using three-electrode setup to indicate the differences in pristine and chemically etched samples, chemically etched and commercially etched as shown in the flow chart in Fig 1.1 below.

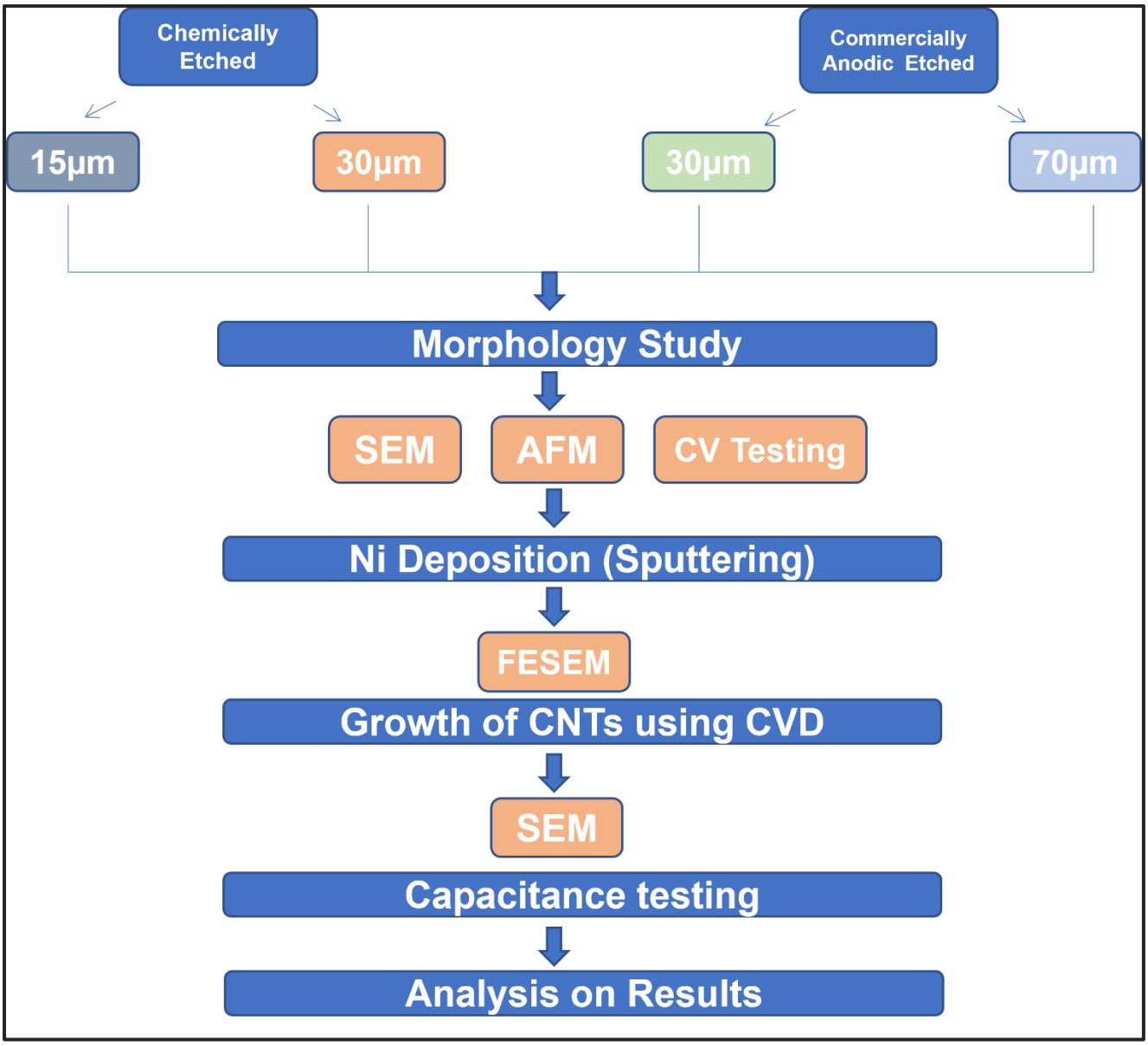

Fig 1.1 Complete flow chart of methodology adopted for this research work

1.3 Thesis Outline

The organization of this thesis research work has been made in different chapters, where each chapter gives the details corresponding to that section.

Starting from chapter 2, gives a detailed background and theoretical overview of supercapacitors with their significant mechanism and applications. Components of current collectors, materials of electrodes including CNTs, Importance of Current collector for the high energy density supercapacitors, the selection of current collector material based on the ideal characteristics of the current collector, Al as current collector substrate, corresponding literature on modification of Al substrate through different techniques for high surface area, and finally the growth mechanism of CNTs and Ni as a catalyst.

Chapter 3, is associated with the experimental methodology and work which includes the selection of substrate, technique for surface modification by changing parameters, sputtering methodology for Ni deposition, CNTs growth process, and finally the characterization tools used in the research.

Chapter 4, corresponds to the results and observations made after the experimental work by using different characterization tools. In the end, all the work is concluded with some drawbacks and future works that can be done on the above research work are mentioned in chapter 5.

2 Theoretical Background and Fundamentals

2.1 Introduction to Supercapacitors

The exitance of double layer is noted since 18th century when Hermann von and Helmholtz first discovered the capacitive phenomena of the double layer in the presence of electrolyte in 1879. At that time he proposed that, by immersing the metallic electrode in an electrolyte it creates a layer of opposite ions around electrode that is electric double layer around, which furthers create a potential difference between electrode and electrolyte [15].

For any energy storage device's performance characterization power density and energy density are key parameters. Batteries have high energy density but lower power density, unlike capacitors. Supercapacitors bridge the gap between batteries and capacitors, by providing a higher power density as compared to batteries and higher energy density than a typical capacitor [16] as shown in Figure 2.1.

Supercapacitors also known as electric double-layer capacitors are storage devices, with the characteristics like high power density, high efficiency, low internal resistance, wide thermal range (-40°C to 70°C), and longer life span as no chemical reactions occur during charging and discharging process. which makes them suitable in the automotive industry to provide acceleration power and regenerative braking [4].

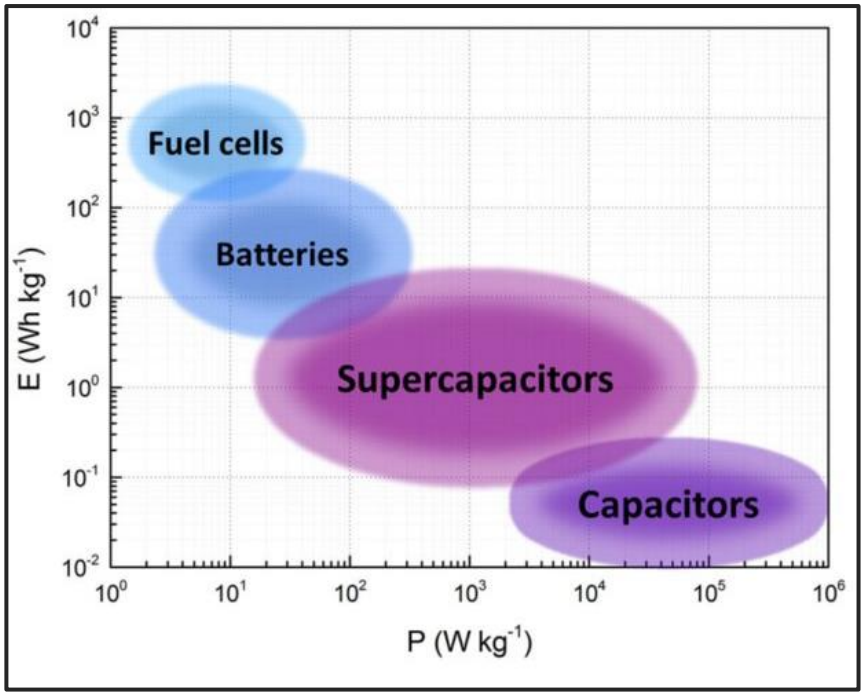

Figure 2.1 Ragone Plot for the typical values of energy and power of different energy storage and conversion devices [17]

When considering the inner mechanism for energy storage SCs are generally categorized into three main groups: Electric Double Layer Capacitors (EDLC), Pseudo Capacitors, and Hybrid Capacitors. EDLC stores the charge either electrostatically or by non-faradic process [18]. when the potential is applied between two electrodes the electrolytic ions are attracted towards the opposite charged electrode. The resultant accumulation of charges on the interface of porous electrode and electrolyte forms a double layer on each electrode known as electric double layer to prevent the recombination of ions at electrodes corresponds to the charged capacitor upon discharging the currents flows and cause decrease in double layer potential. Due to the decrease in Electrostatic forces between the charges the ions are randomly distributed in an electrolyte as illustrated in Figure 2.2. EDLC gives better power performance and cyclic stability, as they can withstand millions of cycles unlike batteries that can withstand only thousands of cycles.

Therefore, there are two contributed capacitances shown in figure below, a simplified SC electric circuit by symbolizing two capacitors in series. The Equivalent Series Resistance (ESR) in circuit accounts for all the resistance that presents in the components of device [19].

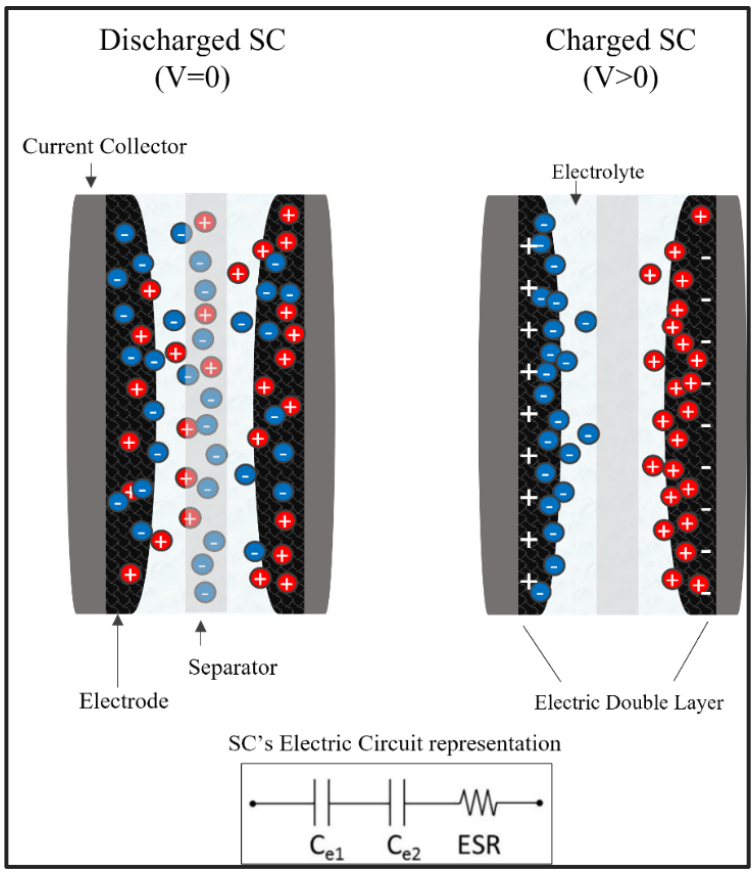

Figure 2.2 Charging and Discharging of SC with an equivalent circuit representation

The capacitance is measured by

$$C = \frac{Q}{V} \qquad 2.1$$

Where C is the one electrode capacitance and Q is the charge transferred at potential voltage V [20].

$$I = \left(\frac{dQ}{dt}\right) = C\left(\frac{dV}{dt}\right) \qquad 2.2$$

Where I is the current and t is the charge time. Whereas the C depends on the distance between electrodes and the area of electrodes.

Pseudo-capacitors involve the faradic process. Upon applying the potential on electrodes the oxidation/reduction reactions occur on electrodes, that happens to provide the passage for charges across double layer and resulting in the flow of faradic current through the supercapacitor. [21].

Hybrid Capacitors combined the characteristics of both EDLCs and Pseudo-capacitors by giving the energy source of battery type electrode and power source of capacitor electrode in the same package. *Components of SC's*, The inner structure of a supercapacitor is based on current collector, active carbon material, an electrolyte, and a separator that works as an isolator between two electrodes. The performance of supercapacitor highly depends on the materials selection of its component.

2.2 Electrodes for Supercapacitors

Active carbon material together with the current collector forms electrode. The electrode of supercapacitor is an electric solid material which performs the absorption and de-absorption of charges. In electric double layer capacitor the capacitance of supercapacitor depends on the surface area of electrode. For EDLC energy storage mechanism different kind of active materials are used for the fabrication of electrodes which involves, Carbon materials, the most known examples of these are CNTs, carbon fibers and graphene[22]. Other prominent electrodes of composite based materials are carbon-carbon composites [23] , composites of carbon conducting polymers [24] etc.

2.2.1 Carbon nanotubes as an active material

For the Electric double layer supercapacitors, carbon material is considered to be more suitable. Therefore, CNTs are now seeking attention of researchers, because of its outstanding properties like enhancement of electrical conductivity of electronic materials [25], mechanical stability, High porosity and surface area which can further improve the electrochemical performance of SC. CNTs are the best suitable solution for technical applications like supercapacitor electrodes. They were first discovered by a Japanese researcher S.Iijima in 1991, since their discovery they have been intense research topic with their potential applications in almost every field [18].

CNTs formed by the single atomic layer of carbon of thin sheet, also known as graphene with the cylindrical type structure of different nanometers diameter. Where each carbon atom create sp^2 hybridized bond with three more carbon atoms. CNTs are further classified as SWCNTs (single Walled CNTs) and MWCNTs (Multi-walled CNTs) based on the fact that how much atom layers are formed from thin sheets as illustrates in Figure 2.3. The disadvantage of CNTs is it's interaction with the living organism and it's unknown consequences.

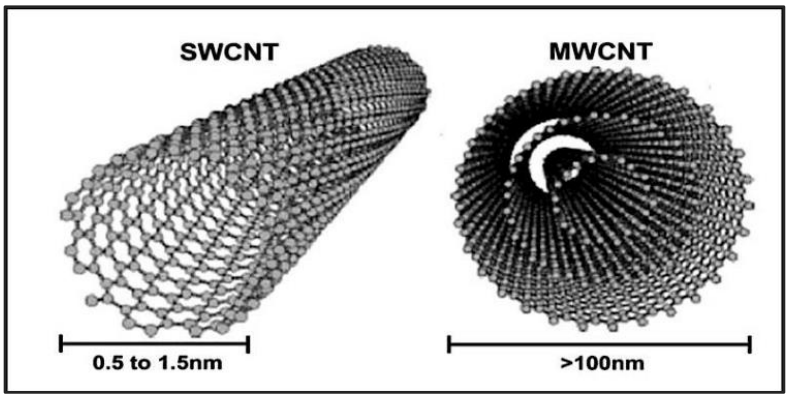

Figure 2.3 Visualization of schematic structure of SWCNT and MWCNT [26]

For the preparation of CNTs base electrodes either the binders are used to load the CNTs on current collector or they are developed as stand free electrodes in both ways it has some disadvantages involves. With binder it can carry the impurities and increase the contact resistance, whereas, in the absence of binder the mechanical stability of CNTs will be compromised. Recently advances have been made to overcome these issues by directly growing CNTs on metallic substrate, which is required to provide the firm support to these CNTs and to exploit the properties of CNTs as current collector [27].

2.3 Current Collector of Electrodes

Current Collectors are the metallic films that are used to support the electrode, also enhance the performance of supercapacitor by transporting the charge from active electrode material to load. However, the contact resistance between electrode and current collector should be minimum to achieve higher degree of charge transportation. Therefore, by improving the surface area of Current collector the activate carbon area can be optimized and higher density can be achieved. Which further increases the power density and decreases the equivalent series resistance (ESR) of Supercapacitor. The internal resistance of supercapacitor is not only determined by the electrical conductivity of electrode but also electrical conductivity of current collector, resistivity of electrolyte, and separator's thickness [28].

The internal visualization of attached current collector with electrode is shown in Figure 2.4 below, the attached current collector is transporting the charges from electrode to external circuit. The

enhancement of current collector's surface area has direct impacts to the active material's surface area which can improve the possibility for storing more charge on its surface.

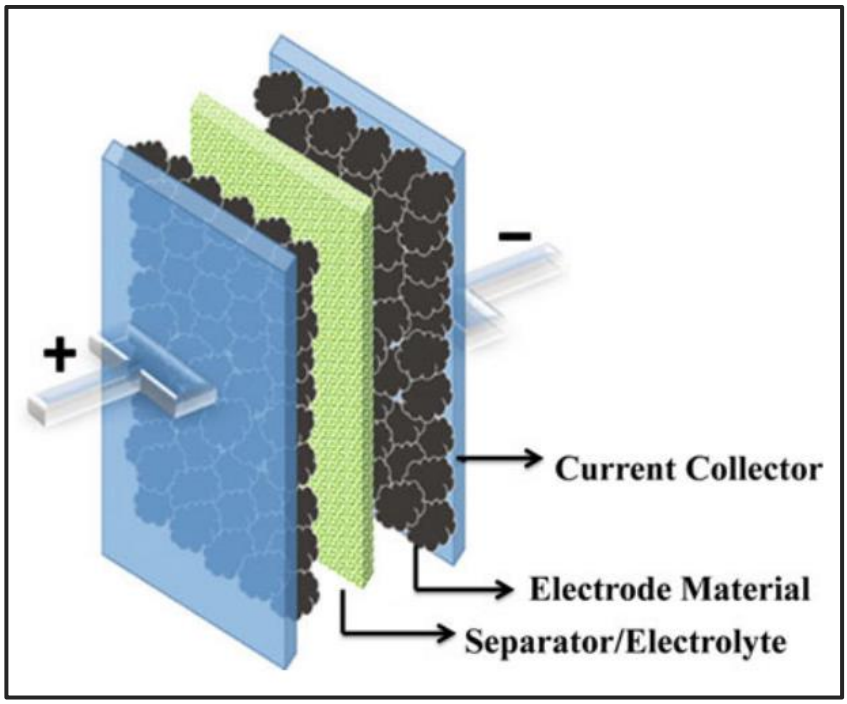

Figure 2.4: Visualization of current collector attached to carbon material in supercapacitor [29]

2.3.1 Characteristics of current collector's material

As an important element of SC, an ideal current collector should have the various characteristics like, high electrical and thermal conductivity, mechanical and thermal stability, good flexibility, high corrosion resistance, high chemical and electrochemical stability, Low contact resistance and strong bonding with electrodes active material, high specific surface area, and most importantly environment friendly and low cost should be considered.

However, for the selection of current collector following criteria should be considered for high efficiency and stability of current collector:

Higher electrical conductivity, is one of the main key element in the selection of current collector, with high conductivity the movement of charges can be maximize to external circuit. With low conductivity of current collector it can cause the generation of heat during charging/discharging process. Another

main element is the low contact resistance between current collector and electrode to enhance the contact area between current collector and electrode. One of main reason for metallic current collectors fame is their low contact resistance property. Many other methods are adopted by researchers which includes the surface modification and deposition of additional layers between interface [9].

Mechanical Strength, of current collector is an important parameter, Since it acts as the supportive substrate to electrode material during the deposition process of electrode and also for the production of supercapacitor cell. During the operation of charging / discharging it gives the firm support to electrode to avoid deformation of electrode material which further can affect the performance of supercapacitor. Moreover, the life span of supercapacitor depends on the mechanical stress bearing ability of current collector which improves the durability and life of supercapacitor , as supercapacitor undergoes various charge and discharge cycles, under numerous harsh conditions causing the mechanical stress on current collector.

Another significant factor in the design of high capacitance performance supercapacitor is the ***optimal density*** of active electrode material on the current collector. The ration between these two materials highly affect the performance of supercapacitor. As by increasing the mass of active electrode material on an inactive component (current collector), can further lead to the decrease in the mass of Supercapacitor cell and increase in the energy density of SC. This situation allows more number of electrode material to agglomerate at certain area of space. However, the optimization of weight should be done properly to escape the chance of mechanical and electrical un-stability of current collector.

Cost & Sustainability, are the most considerate factors for the commercialization of supercapacitor. In terms of cost, material's affordability, availability and also easy to fabricate should be consider while choosing the material for supercapacitor to make it cheap, and easily available for consumers. While In terms of sustainability, it is equally important to choose the environment friendly materials that can be reused and recycled. These steps significantly reduced the impact of materials and device usage on environment without causing any serious harm to the nature [30].

2.3.2 Major materials for the current collectors

As it is already discussed that the electrode material is deposited all over the surface of current collector either by growing the CNTs or carbon fibres on it, or by using binder to paste graphene based electrodes on it. Hence, the conjunction of current collector and electrode plays the significant role in the charge transfer and power delivery rate to external circuit. Therefore, various materials are used as current collectors with varying native properties of it. Selection of material should be made while considering that the current collectors doesn't react with the electrode or electrolyte material or it can affect the performance of supercapacitor. Various materials are used with various characterisations like, carbon cloth with the good electrical conductivity but low mechanical strength, stainless steel can also be used with its renowned properties like good thermal and electrical conductivity, high mechanical strength but this would made the device bulky. Other famous metallic materials Ni, Al, Ti, Ag, Nb and Cu have also been found in the literature [12] [13].

Carbon Based Materials, are light weight based current collectors, that have the features like good flexibility and lower contact resistance between the current collector and active electrode material [31]. Since the storage device's rigidity makes it impossible to use in flexible and wearable applications. Therefore, for the flexible electronics the use of bendable current collector is important. Carbon based fabrics and polymers are most prominent materials with the uttermost characteristics like good electrical conductivity, better mechanical strength and bendability.

Carbon paper is the carbon based material used by P. Luio [32], where he demonstrated the usage of carbon paper based current collector for graphene hydrogel (GH) based electrodes. These GH electrodes are thermally grown on the carbon paper current collector. Below, Figure 2.5, shows the high porosity of GH electrodes using SEM and TEM images. Due to high porosity and better electrical conductivity of these electrodes using carbon paper current collector, they shows the better rate performance at the current density of about1.18 A/g with the specific capacitance of electrodes was up to 294 F/g.

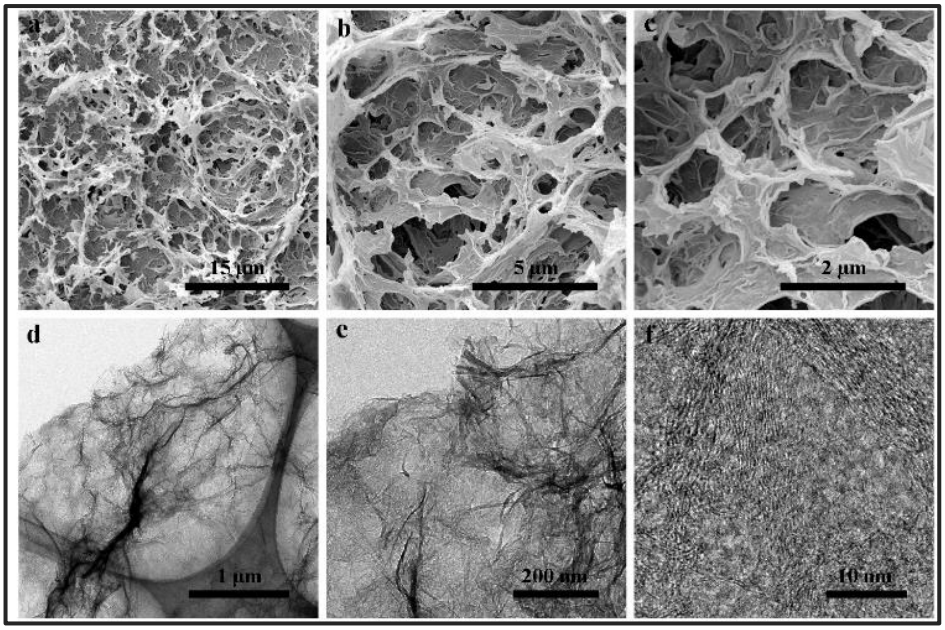

Figure 2.5: SEM (a-c) and TEM (d-f) images at different magnifications of GH Morphology [32]

Another promising carbon based current collector material used is Carbon nanotubes (CNTs). [33] Uses a simple printing technique using screen printed poly(3,4- ethylene dioxythiophene)-poly(styrene sulfonate) (PEDOT:PSS) ink with an addition of Multiwalled CNTs. These ink composites were printed on the filter paper substrate, and used as both electrodes and current collectors. Later assembled as supercapacitor using these electrodes, electrolyte and separator, assembly shown in Figure 2.6 below. Almost after running 1000 cycles, this device exhibits the retention of up-to 70% with the specific capacitance of almost 20.3F/g. Overall, this paper based current collector is the environment friendly, low cost and flexible with the better rate performance supercapacitor.

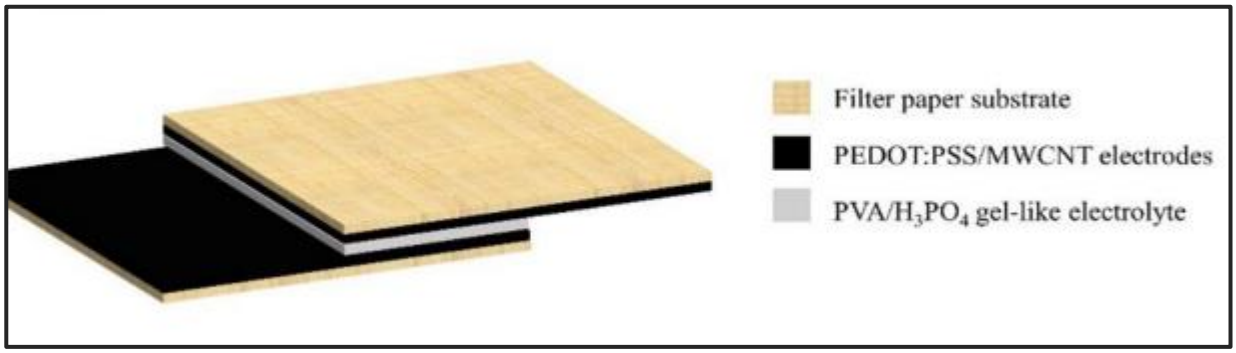

Figure 2.6: Supercapacitor schematic illustration to show the assembly and architecture of SC [33]

Similarly other prominent carbon based material is graphene uses in the form of printing technology same as previously described and other is laser writing method to increase the porosity of electrode surface to increase the capacitance of supercapacitor device by using stand-alone electrodes without current collector [34] [35].

Metal Based Materials, are the famous and most used current collector materials in the application of supercapacitor device. Some of the common metals, Nickel, steel, Aluminium , Titanium, Copper, Platinum and gold are most frequently used materials as current collectors. The main disadvantage of these metallic based current collector is it's limitation with corrosive electrolytes. For the corrosive electrolytes Au is being used which is an expensive material, but increases the price of device [36].To compensate this limitation various advances and researches have been made to use the aqueous electrolytes without causing any harm to metallic current collector, in comparison other organic electrolytes, water in salt are also being used resulting in the usage of high power density up to 10kW/h. For this purpose literature has shown the usage of corrosion resistant materials and use of conductive composites of metals and active carbons with the modifications on current collector surface are used.

As after the certain number of charging/discharging cycles, the carbon layer from flat surface of metals start peeling off due to bad adhesion between electrode and current collector in the presence of organic electrolytes resulting in the declined electrochemical performance of supercapacitor.
In this thesis the proposed metallic current collector is an Aluminium substrate, therefore the next section is dedicated to the detailed study of an Al as a current collector material.

2.4 Aluminium as the Current Collector

For the recent few years, Al has gained particular interest as current collector material in the fabrication of Supercapacitor with the significant impact on the cyclic stability and electrochemical performance of SC. It is an important point to note that the current collector substrate for high performance supercapacitors plays an important role, as it carries the structural foundation of supercapacitor by carrying the nanocomposite carbon based electrodes.

Al is the abundant metal on earth which can help to fabricate low cost energy storage supercapacitors. Al foils are made from aluminium alloys with 92 to 99% purity, with varying the thickness of foil and melting point of 660°C. There are various advantages of using Al substrate other than cost effectiveness as compared to other metals they have good electrical and mechanical properties which are perfectly suitable for the charge transfer and electrochemical reactions. Also they have chemical stability in organic electrolytes. The ductility of Al foil to allow it to use in different packaging techniques of supercapacitors. Moreover, during the fabrication of Al foil this is exposed to the air which causes the presence of nascent oxide layer on Al foil, which means it doesn't require any extra modifications like pre-deposited buffer layer, this simplifies the preparation steps of current collector [37]. Al as compared to other metals Ag, Cu and Ag gives the lower internal resistance. Moreover the density of Al metal (~2.70g/cm^3) is lower as compared to other metals , which makes it an ideal substrate to decrease the mass of energy storage supercapacitor.

2.4.1 Modification of Al surface

Since the morphology interaction of electrode active material and current collector decides the important factors like power delivery rate, efficiency for taking out the stored energy from electrodes [38].Further modifications of Al substrate can be made to overcome two problems that can be caused by the smooth metallic surface, firstly the modifications on Al substrate can cause the hierarchical micro and nano structure on surface which can improve the adhesion between current collector and electrode. Secondly, the increased surface area can provide more area to grow or deposit active carbon electrodes e.g, CNTs. More specifically in the case of EDLC, better bonding between the current collector and CNTs can prevent the loss of CNTs during the fabrication process and leads to the high rate electrochemical performance in practical application of SC. Strong interface between the two materials reduced the delamination in harsh conditions and improves the life of device [39].

An analysis of available literature has made to show how the advances have been made in the nano-structuring of Al foil to prevent the adhesion based problems with providing more surface area on Al current collector and their impact on the electrochemical performance of supercapacitor.

Among the modification methods physical treatment of metallic current collectors is the most used method, one of the famous technique is etching. This process has various applications found in

literature from ancient times for making jewellery to reducing the weight of materials e.g. aircraft wings.

Etching is the corrosive technique applied by using chemicals on materials to shape the materials or cause some hierarchical structuring on the surface of metals. ***Chemical etching*** or ***Wet etching*** is one of the etching process that is carryout out by using acids or chemical solutions also known as **etchants**, to remove the material from the substrate. Wet etching involves three main steps of reactions, (1) first step involves the diffusion of the etchant solution to the targeted material or structure (2) chemical reaction happens between the etchant acid and the material to be removed (3) the formation and diffusion of by-products in result of reaction with the etched away surface. In the result of etching the material can be removed in two ways; ***isotopically (uniformly in all directions)*** or ***Anisotropically (uniformity in just vertical direction)*** [40].

[41] Has studied the chemical etching of Al using the 1.25 mol Ferric chloride ($FeCl_3$) etchant, where the effect of etching time and temperature are explored with respect to etch rate and depths of etched pits. Figure 2.7, illustrates the experimental setup normally used for the chemical etching of the substrate, as it can see from the figure this procedure does not require any complex setup, it is cost effective procedure.

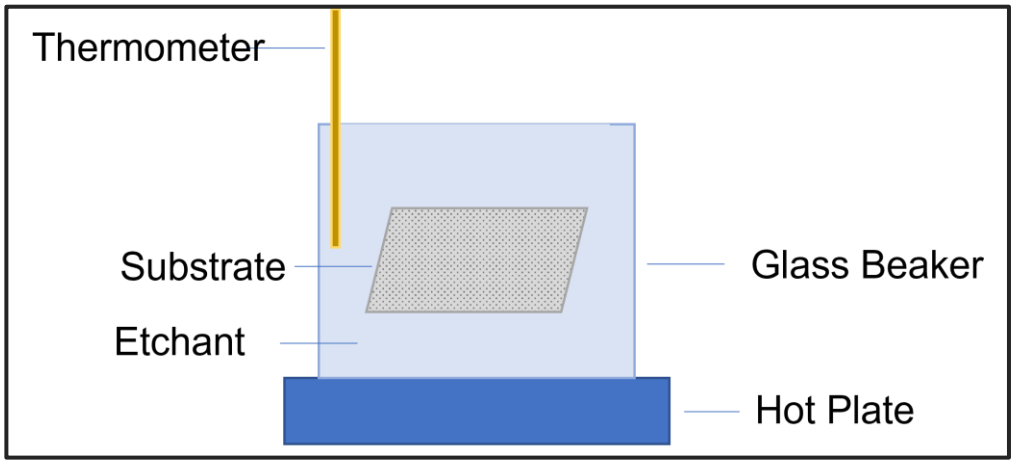

Figure 2.7 Experimental Setup for chemical etching

Similarly, [42] has investigated the three different surface roughening technique to introduce micro-structures on Al surface: boiling water, HNO3/HCl etching, and HF/HCl etching. The following

experiments has been done to tailored the hydrophilic nature of Al alloys, first by surface roughening second by chemical salinization on Al surface. The etched surfaces are than further characterised by suing Atomic Force Microscopy (AFM). The roughness parameters depends on the technique used, however, all the three methods successfully exhibits the micro and nano structure on Al foils.

In addition to the traditional chemical etching process, another alternative technique of etching using electric current is introduced in recent studies to etch the semiconductor materials and metals. This process of etching is known as ***electrochemical etching*** or ***Anodic etching*** which is facilitated by the galvanostat or potentiostat to provide the required electric charge for etching**.** The electric field leads to the induction of oxidation potential, and form the oxide layer on top of material surface, which is further get dissolved by the etchant and in the result the targeted material is removed. The main advantage of this process is, it provides the great control on etching rate and etched features that includes the direction and size of microstructures also offers the fabrication of complex structures by controlling the current or potential [40]. In the literature electrochemical etching is described as the commercial etching process to produce Al current collectors for EDLC's, as it can be used to etch wide range of materials and metals.

Reng-Gui [43] Have studied the DC electrochemical etching to produce the Tunnel like morphology of etching technique, known as Tunnel Etching. The experiment is carried out by using commercial Al foil as anode electrode, and graphite as counter electrodes with an electrolytic solution of H_2SO_4 and HCl by changing the temperature of electrolyte. The experimental setup can be visualized in Figure 2.8. Here the Capillary tube is used to measure the surface tension, the height of capillary directly ascends by the electrolyte which shows the impact of temperature on surface tension of electrolyte. The results exposed that by varying the temperature the density of tunnels increases with the increased tunnel length.

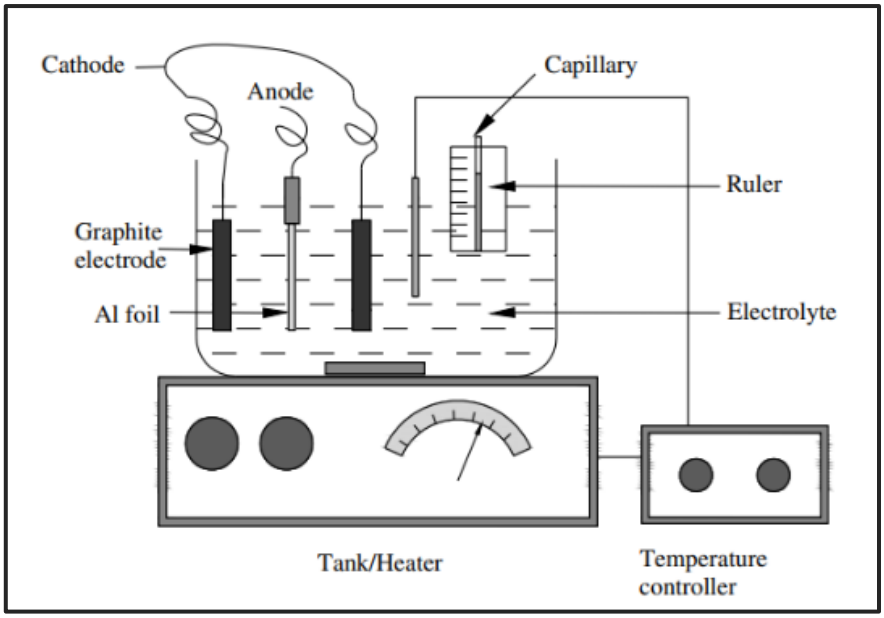

Figure 2.8 DC Etching of Al experimental setup [43]

Laser treatment is another surface roughening technique that is scarcely reportedly in literature, an efficient way to create homogeneous micro-structures on current collector surface to increase the surface area of metal. D. Yang and A. Laforgue [44] adopted the laser roughening technique. The proposed technique was explored by varying the laser intensity and power to control the size of pits on 50µm mounted Al foil inside the vacuum chamber under high vacuum conditions. The incoming laser beam was scanned all over the Al surface to roughen with the scan rate of about 200mm/min. Further the supercapacitors assembled with microstructure Al foil was evaluated based on its electrochemical performance which provides cyclic stability on CV curves . The results demonstrates that the laser ablation techniques with its flexibility to control the microstructures on Al gives the promising surface enhancement with oxide free current collector surface for supercapacitors.

2.5 CNTs Growth Mechanism

For the growth of CNTs various synthesis methods are used i.e. laser ablation, Chemical Vapor deposition (CVD) and arch discharge. Among the above defined methods, CVD is the most investigated and frequently used method to synthesize CNTs, because of its's advantages like requirement of simpler setup and equipment, mild working conditions e.g. temperature and pressure, more suitable for large mass production of CNTs.

APCVD setup is illustrated in the Figure 2.9, the synthesis of CNTs inside the CVD furnace involve the decomposition of carbon from the carbon containing gas (alcohol, hydrocarbons) on the transition metal catalyst surface. The synthesis process carried out at the temperature of 500 to 1000°C depends upon the melting point of substrate. This procedure allow the dense growth of CNTs on substrate. The growth rate of CNTs is greatly influenced by the numerous factors such as ; reaction conditions, gas composition, precursor gas, deposition time, substrate morphology and catalyst used. Extensive studies have been made on the effect of catalyst, temperature, synthesis process and gas compositions [45] [46].

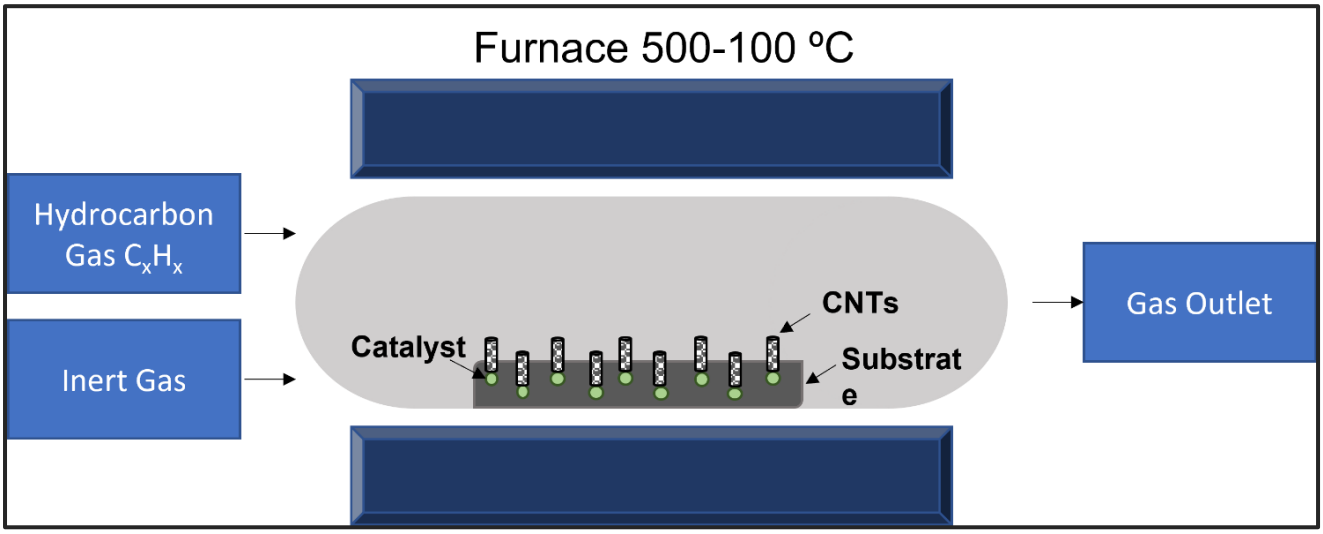

Figure 2.9 CVD setup for Synthesis of CNTs which is further used in this research study

Catalyst is describe as the material that enhanced the chemical reactions during any process and avoid their consumption. For CVD synthesis it is assumed that upon introducing the hydrocarbon gas into the reaction chamber these gas particles get absorbed by the catalyst nanoparticles available on the substrate, where they catalytically decomposed the hydrocarbon gas into carbon species. These carbon atoms are diffused and transported through the catalyst and gather on the catalyst surface, as the process proceeds more and more carbon species get accumulated to form cylindrical nano tubes. Fe, Ni and Co are among the most used and successful transition metals that are used as catalyst for directed growth of CNTs [47].

Ni is used as catalyst as it has the various characteristics i.e., it is abundant element on earth, it has the high melting point of about (1455°C), which makes it viable to heat the catalyst at high temperature for CNTs growth, it has great affinity for carbon atoms [48]. Similarly, [49] has used Ni as a catalyst on bulk Cu substrate for its capability to attain more directed and dense CNTs growth, with the conclusive results that thinner catalyst films grow more vertically thin aligned CNTs as compared to thick films as they can form more thick islands of Ni and hinder the CNTs growth.

3 Materials & Methods

3.1 Fabrication of Microstructured Al Substrate

Selection of substrate, is made by using the available pristine Al foil of two different thicknesses (15µm and 30µm) of 90.0 to 95.5% pure Al which are commercially purchased from VWR. The two other commercially anodic etched foils (FOILTEC, 70µm and 30 µm) are used to make a comparative study for chemically and anodic etched samples.

The experimental study of chemical etching is consist of two main steps cleaning and etching of the substrate. The preparation of sample is carried out by employing the meticulous processing steps in order to ensure the reliability and reproducibility of results for the fabrication for micro-nano structures on Al foil. The samples from Al foil are cut precisely to dimension of 4 X 4 cm^2, and subjected to the thorough cleaning of samples by following sequential immersing approach to remove the unwanted contaminants which includes the oil grease and heavy oxide. Where the Acetone is used as the cleaning agent , because of its tremendous solvent properties and its ability to eliminate both organic and inorganic impurities. Initially, the samples were immersed inside the acetone for about 5 minutes to eradicate contamination, and then samples were washed thoroughly with DI water to purify the samples further by removing any acetone residuals following by the Nitrogen to dry the samples.
Various etching sessions by following the same procedure have been conducted to gather the samples to check repeatability.

Error! Reference source not found., summarizes the details of samples used for this research study, all the samples were denoted by prefix 'Al' denotes the Aluminum, followed by the numbers present the thickness of Al foil and the letters indicate the nature of this foil e.g. Al-30CE shows the foil is chemically etched.

Table 1 presents the nomenclature and detail for Al foils used

Al-15p	*15µm* pristine foil
Al-15CE	*15µm* Chemically etched foil
Al-30p	*30µm* pristine foil
Al-30CE	*30µm* Chemically etched foil
Al-70	*70µm Anodic Etched foil*
Al-30	*30µm Anodic Etched foil*

3.2 Chemical Etching of Al Foil

The employed chemical etching process in this study has utilized the commercially available Al etchant (ANPE 80/5/5/10, Microchemicals) with the acid composition comprises of H_3PO_4 :HNO_3: CH_3COOH and H_2O (73% : 3.1% : 3.3% :20.6%). The selection of this etchant was made while considering the factor, i.e. this etchant is considered to be less hazardous as compared to the commonly used acid based etchants HCl and H_2SO_4. Furthermore, the availability of this etchant in the laboratory was also taken into account while selecting. Generally, the Al etching is highly exothermic. The etching starts by the Nitric acid (HNO_3) which prepares the substrate by oxidizing the surface of Al to remove any contaminants might present on surface, followed by the primary etchant phosphoric acid that dissolves the oxidation layer (Al_2O_3) of few nm on the Al surface, and further the acetic acid (CH_3COOH) aids in the buffering to Al etchant by wetting the surface of Al. Water dilutes the etchant to control the concentration of etchant by adjusting the etching rate at a certain temperature.

The following reaction for primary etchant can take place:

$$2H_3PO_4(l) + 2Al\ (s) \rightarrow 2AlPO_4(s) + 3H_2O\ (g) \qquad (R3.1)$$

The initial study was commenced by immersing the pristine Al samples namely Al-15p and Al-30p individually inside the petri dish containing 50ml solution each as shown in the Figure 3.1(a) and (b), the etching temperatures 20°C to 30°C with an interval of 5°C were used. The double-sided etching process for Al-15p and Al-30p was initiated at 20°C. In the case of Al-15p the etching was performed for 5, 10,15 20 mins, it was noticed that the sample starts vanishing after approximately 21 minutes as shown in Figure 3.1(c). Consequently, the etching was stopped at 20 minutes. During the etching trial of Al-15p, it was observed that the sample's etching commenced after 5 minutes, therefore for Al-30p substrate was etched from 10min. Hence, for the Al-30p specimen, the thickness of 30μm was sufficient enough to withstand the etching for approximately 30 minutes. Therefore, the etching was meticulously performed for 10 to 30 mins, with an interval of 5 mins.

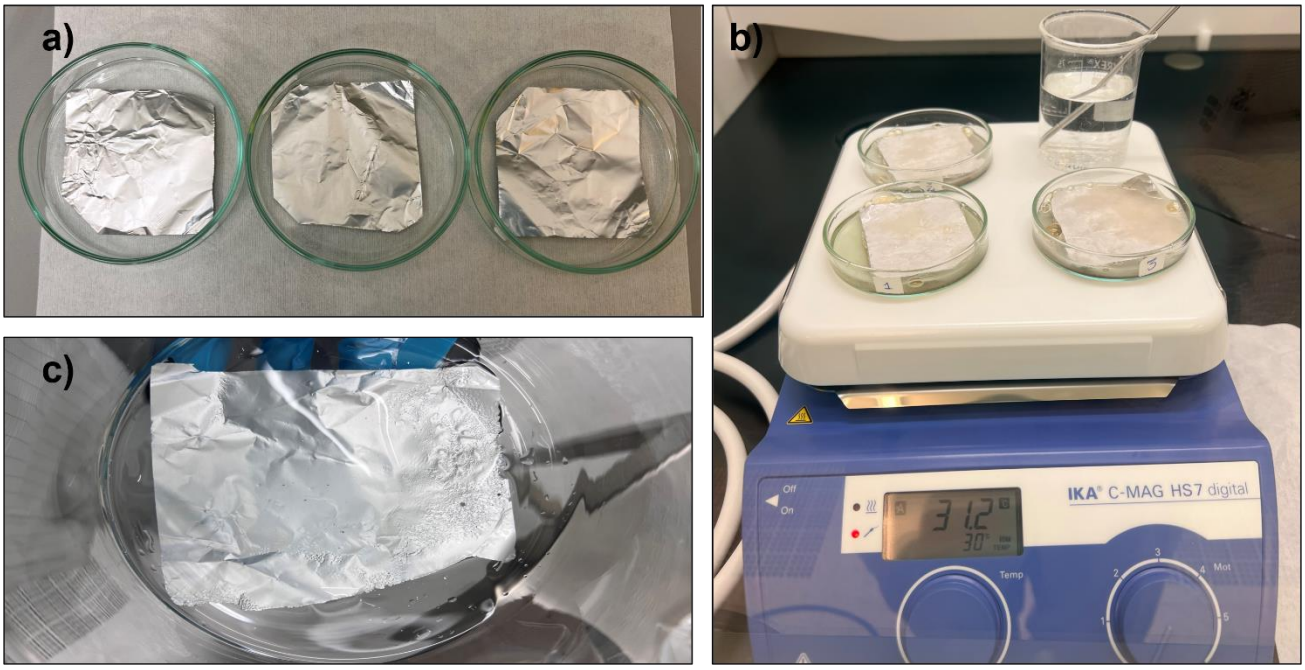

Figure 3.1 Chemical Etching samples setup, and the dissolution of the sample after etching for longer time

Subsequently, the next trial of etching was conducted at 25°C, in the previous way both samples of Al-15p and Al-30p were immersed inside the etchant solution of the same volume. The etching for Al-

15p was observed with the 5 and 10 minutes of etching to prevent any damage to the foil. Similarly, for Al-30p the etching experiment was terminated after 20 minutes of etching, with the total 4 samples of Al-30p etched at 5,10,15, and 20 mins.

Lastly, the etching was performed at 30°C, where the etching time for Al-15p was 5 minutes and for Al-30p the etching duration was 5 and 10 minutes, respectively. Table 8 in the appendix provides a concise overview of the adopted etching parameters for Al-15p and Al-30p. Upon completion of etching experiments on Al-15p and Al-30p, the selective samples were further subjected to qualitative and quantitative analysis. Afterward, one sample with the optimized pits dimension was selected from each set of etched samples to proceed with further experimental work and analysis.

3.3 Synthesis of CNTs Using the CVD Process

The selected samples from the chemical etching process, Al-15CE(20, 10mins) and Al-30CE(25, 5mins) were further used for the deposition of Ni catalyst to assist the CNTs growth, along with Al-15p, Al-70, and Al-30 substrates. The Ni of 10nm Ni thickness was deposited by my class fellow Hamza using a DC magnetron Sputtering machine (Sputter AJA, ATC 20x20x30). The Ni nanoparticles were deposited under 25W of DC power, with an Ar flow of 15sccm, pressure set to 1.08×10^{-2} rotation speed set to 10 R/s.

Prior to the sputtering process, all the samples were processed through the proper cleaning process using isopropanol and DI water. The samples were initially immersed inside the beaker containing Isopropanol to get rid of any grease or contaminants on sample's surface for around 5 minutes. Later the samples were rinsed and washed with DI water and dried by using Nitrogen gun. To facilitate simultaneous sputtering conditions to all the samples, the samples were cut to the dimension of 2 X 10 cm^2, and were affixed to the stage in a way that all the samples were able to be clipped there, and extended support is provided by using tape as shown in Figure 3.2 below.

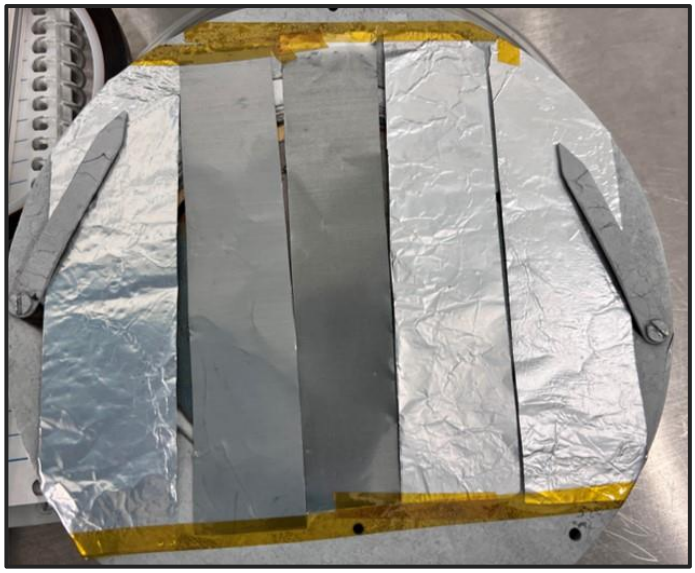

Figure 3.2 Illustration of samples arrangement on sample stage for uniform sputtering exposure

Now the deposited samples named as Al-15CE, Al-30CE, Al-15p, Al-30, Al-70 were prepared for the deposition of CNTs. After the deposition of 10nm Ni thickness on Al foil, the synthesis of CNTs is performed by using the CVD setup (Tube Furnace High Temperature 2-MSL, MTI Corporation). The samples were cut of 1.5 X 2cm^2 to affixed on the quartz stage. For CNTs growth pristine foils Al-15p, Al-30p and chemically etched foils Al-15CE, Al-30CE, Al-30, and Al-70 were used as shown in Figure 3.3(d).

The synthesis was carried out inside the quartz tube of 60cm long, 4.3 cm ID(inner diameter). The placement of samples inside the tube was made by using a small quartz dish with the customized Si wafer stage was used as the sample holder, which was precisely placed in the center of quartz tube by the help of rod in the accurate heating zone of tube. The tube is filled with the inert and hydrocarbon gas, in this experiment Ar is used as inert gas and also carrier gas , and C_2H_2 is consumed as hydrocarbon gas. The CVD experiment was conducted using the working temperature 600°C and gas composites comprises of Ar: H_2: C_2H_2 with an optimized gas composition 40: 100: 20 from my fellow Tasfia.

The desired temperature was achieved in 58 minutes with the continuous 40sccm Ar flow, following the procedure further by introducing H_2 and C_2H_2 into the reaction chamber to start synthesis. While the APCVD process, the Ar as a carrier plays an essential role by facilitating the flow of 20sccm C_2H_2

to the reaction chamber, upon entering the reaction chamber hydrocarbon gas undergoes thermal decomposition to form carbon that further dissolve onto the Ni catalyst's surface. Here 100sccm H_2 is supplied for reduction and etching of Ni nano particles. After the carbon reaches to certain concentration level it starts forming a semi fullerene cap which provides the base structure for the successive growth of cylindrical CNTs. The CNTs continuously to grow upon the continuous supply of carbon from the decomposition of acetylene on to the Ni catalyst that could be a tip growth or bottom growth. The synthesis time lasted for 15 minute. The whole synthesis procedure was assisted by water vaporization to enhance the purification of CNTs and avoided accumulation of amorphous carbon by activating the catalyst for longer time [51].

Upon the completion of synthesis of CNTs, 300sccm N_2 of flows into the reaction chamber to facilitate the cooling of furnace., and the CVD chamber was cooled down to room temperature.

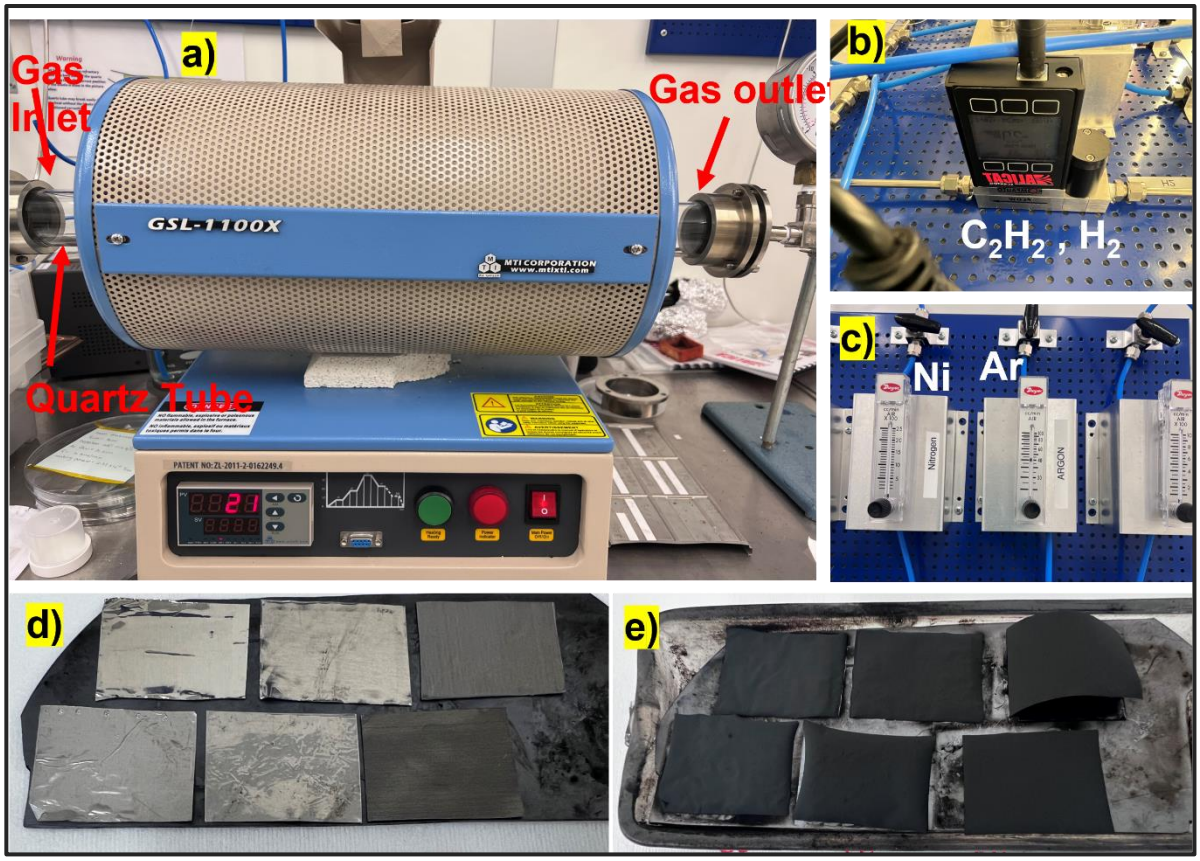

Figure 3.3 Illustration of CVD setup and experiment a) CVD furnace (b) (c) Gas Flowmeters (d) arrangement of samples on Sample stage before CNTs growth (e) samples after CNTs growth

3.4 Characterization Tools

3.4.1 SEM & FESEM for morphology analysis

Scanning Electron Microscopy (HITACHI,SU 3500) and Field Emission Scanning Electron Microscopy (HITACHI, SU 8230) is used for the morphology analysis. Scanning Electron Microscopy works on the principle of detection of reflected electron beams from the specimen. The electron source is the main element of SEM, in most cases hot tungsten filament is used as the electron source. Upon heating it provides more energy to the electrons which are further guided towards the specimen by anodic plates and condenser. After electrons hit the sample they reflect in random directions and get detected by the detector. The accelerating voltage determines the penetration of electrons depth into the specimen surface. The advantage of using SEM as compared to optical microscopy is its High-resolution result, thermionic SEM(SU 3500) offers magnification from 5 to 300,000X with an accelerating voltage of 0.3 to 30kv Whereas, FESEM (SU 8230) has magnification up to 1,000,000X.

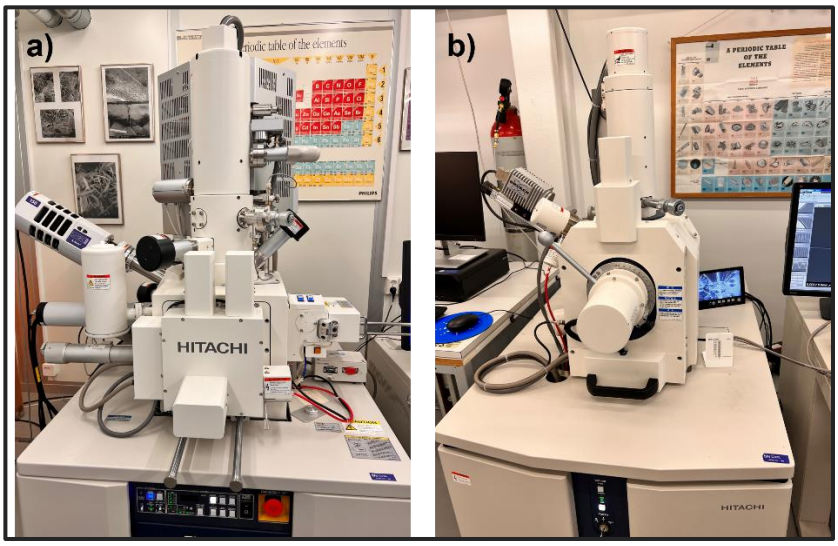

Figure 3.4 HITACHI -Scanning Electron Microscopy for a) FESEM (SU 8230) and b) SEM (SU 3500)

3.4.2 AFM for surface roughness statistical analysis

Atomic Force Microscopy (AFM XE 200, Park Systems Co.) is used for the quantitative analysis of the samples to measure the roughness of Al specimens. Unlike scanning microscope that depends on electron emission and reflection, AFM works on the principle of scanning the AFM probe by scanning

the sharp tip over the sample. In AFM, it gives the 3D profile by measuring the force between the sharp tip(<10nm) and the specimen from a very short distance of up to 0.2 to 10nm.The scanning resolution for AFM is 5 to 10nm (Laterally) and sub-nanometer vertically. This sharp probe is supported by the cantilever, and to maintain the force equally the cantilever is deflected constantly. As the probe moves over the sample's feature, the cantilever deflection is further tracked and directed towards the photodiode detector. by the laser beam Below the figure shows the working principle and setup for AFM XE 200. There are three basic working modes of AFM , Contact Mode, Tapping and Non-Contact Mode.

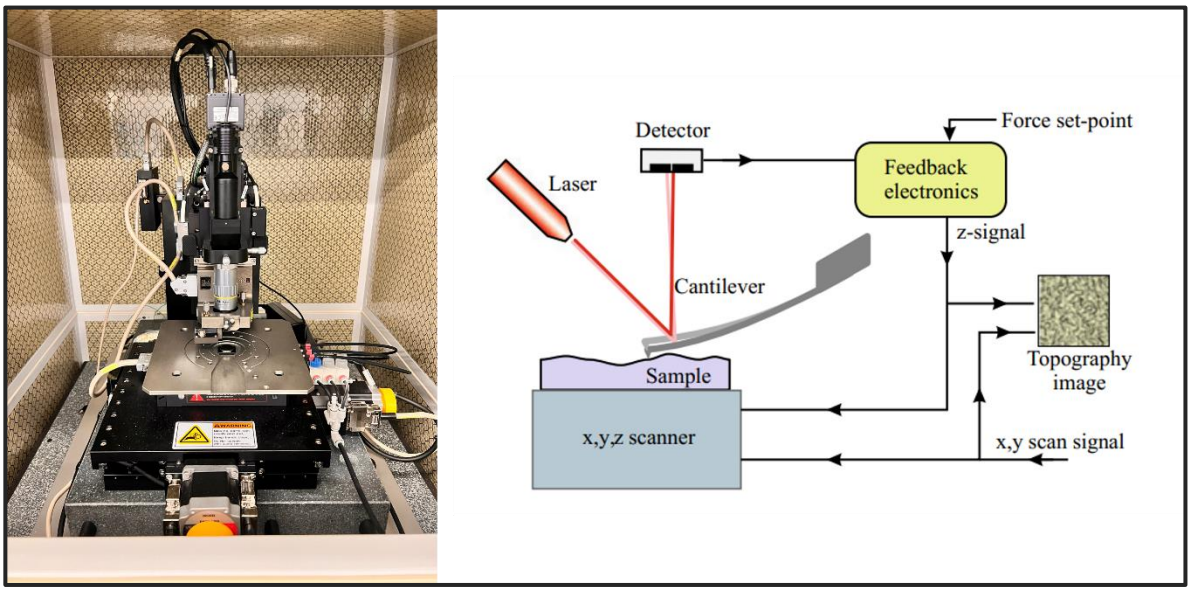

Figure 3.5 Illustration of AFM XE200 setup and working principle diagram of AFM[52]

For contact mode, cantilever uses the constant force for the interaction of probe tip and sample. In tapping mode, the cantilever oscillates the tip on sample at the certain resonance frequency. Whereas, in non-contact mode the distance between the sample and tip is maintained and the interacted forces between tip and specimen are measured this mode is useful for samples which are sensitive to contact and can cause damage to samples. This study has made analysis based on non-contact mode.

The important roughness parameters in AFM are average roughness of surface R_a, and root mean squared roughness R_q, which are more commonly used to describe the quantitative features of sample.

Which are mathematically determined as

$$R_a = \frac{1}{n}\sum_{i=1}^{n}|Y_i| \qquad 3.2$$

$$R_q = \sqrt{\frac{1}{n}\sum_{i=1}^{n} y_i^2} \qquad 3.3$$

3.4.3 Electrochemical workstation for characterization of electrochemical performance

An electrochemical workstation (**VSP-300, SN. 0542, Bio-Logic SAS**) is used for the electrochemical characterisation of pristine, etched and CNTs grown foils to measure the capacitance. The three electrode setup consists of reference electrode, counter and working electrode. Reference electrode is with known redox potential. Here graphite is used as counter, Ag is used as reference and Al samples are used as working electrode. The capacitances are measured on Al-15p, Al-30p, Al-15CE, Al-30CE, Al- 30, Al-70 and CNTs grown on all these samples. The voltage scan of 100mV/s is applied between the working and counter electrode within the potential window of 0.8V, with the aqueous 1M sodium sulphate electrolyte(Na_2SO_4) as it is the salt based and non-toxic, for CV analysis to measure the specific capacitance.

$$C = \frac{Absolute\ area\ under\ the\ curve}{2 \times potential\ sweep\ rate \times working\ potential\ window} \times 1000 \qquad 3.4$$

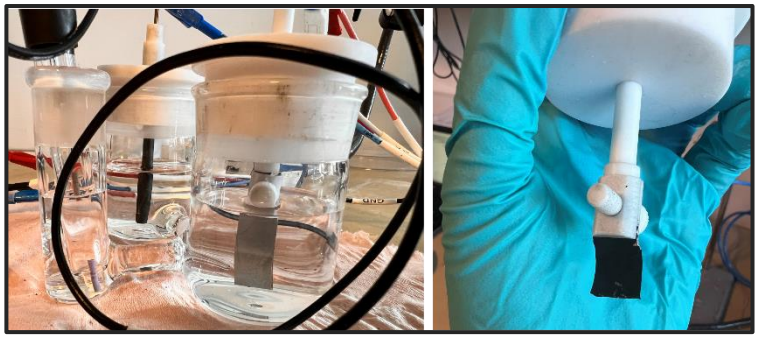

Figure 3.6: Visualization of 3 electrode setup based on Counter Electrode, Working Electrode Reference Electrode

4 Results & Discussion

4.1 Morphology Analysis of Chemically Etched Al Samples

All the conditions experimented with, for the pristine Al foil are further characterized to analyze the morphology and microstructures.Figure 4.1, exhibits the surface morphology of pristine Aluminium specimens Al-15p and Al-30p. The figures reveal the surface features such as crumbliness, rolling lines, and small pits-like features (circled) resulting from the manufacturing process.

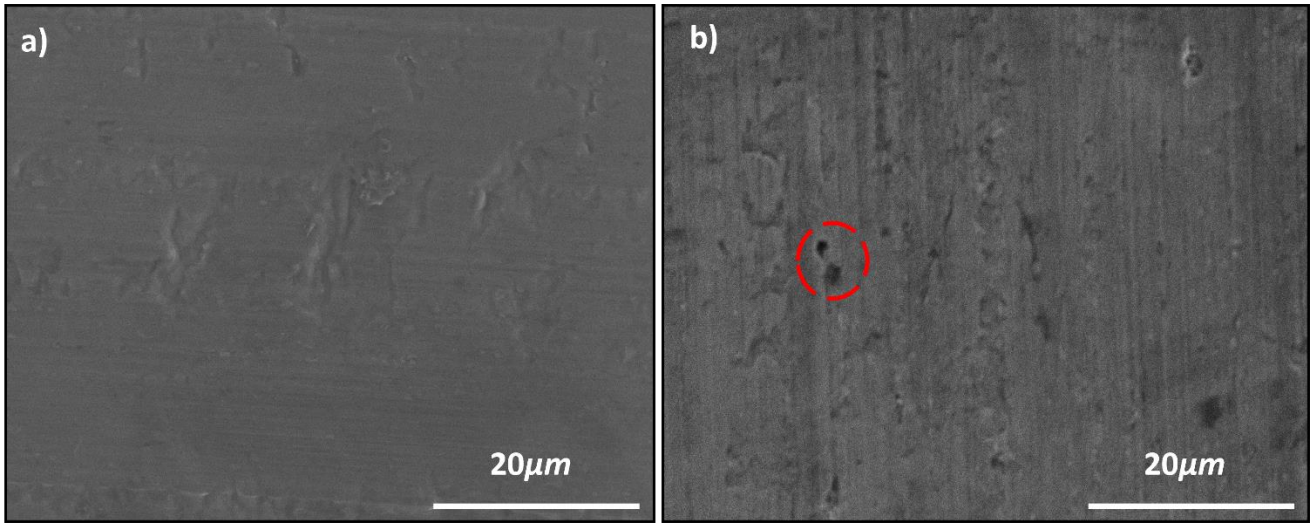

Figure 4.1 SEM Morphology of pristine Al foils a) Al-15p and b) Al-30p with the manufacturing resultant pits, captured at the magnification of 2k, 10kV acceleration voltage

The successful results were achieved after etching Al-15P & Al-30P using ANPE Al etchant. The etching for both foils was performed at 20°C, 25°C, and 30°C as illustrated in Figure 4.2 & Figure 4.3. Through the comparison between the morphology of pristine Al foil (Figure 4.1) ,and chemically etched samples, notable observations are concluded. Prior to etching the foil, the surface of Al appeared to be smooth without any considerable marks of micro or nanostructures. Conversely, after going through the etching process, the samples display some significant micro-structures of granular-plate like erection.

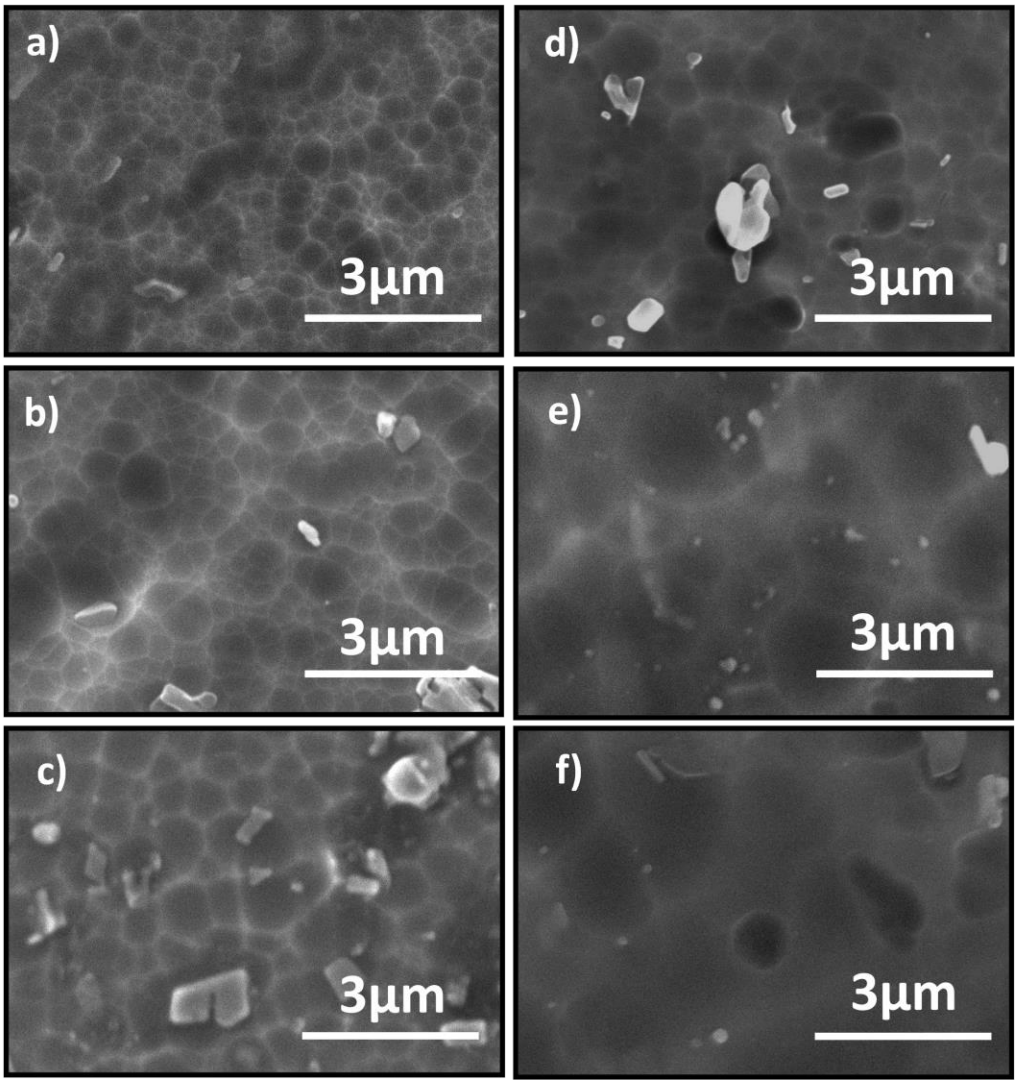

Figure 4.2 SEM images of chemically etched Al surface (15µm) etched at 20°C for (a) 10mins (b) 15 mins (c) 20 mins, 25°C for (d) 5mins (e) 10mins, and 30°C for (f) 5mins

The resultant structure of etching highly depends on the composition and concentration of etching. The ANPE Al etchant utilized in this experimental work, causes the micro and nano level granular-plate type circular structure. This Al etchant due to its composition attacks the crystallographic planes, that causes equiaxed grain like structure. Most of the studies in literature have been made by using hydrochloric acid that is very strong acid which aggressively attacks on the higher energy areas mostly the rolling boundaries or dislocations as a result induce large cubic or rectangle type irregular cavities [53].

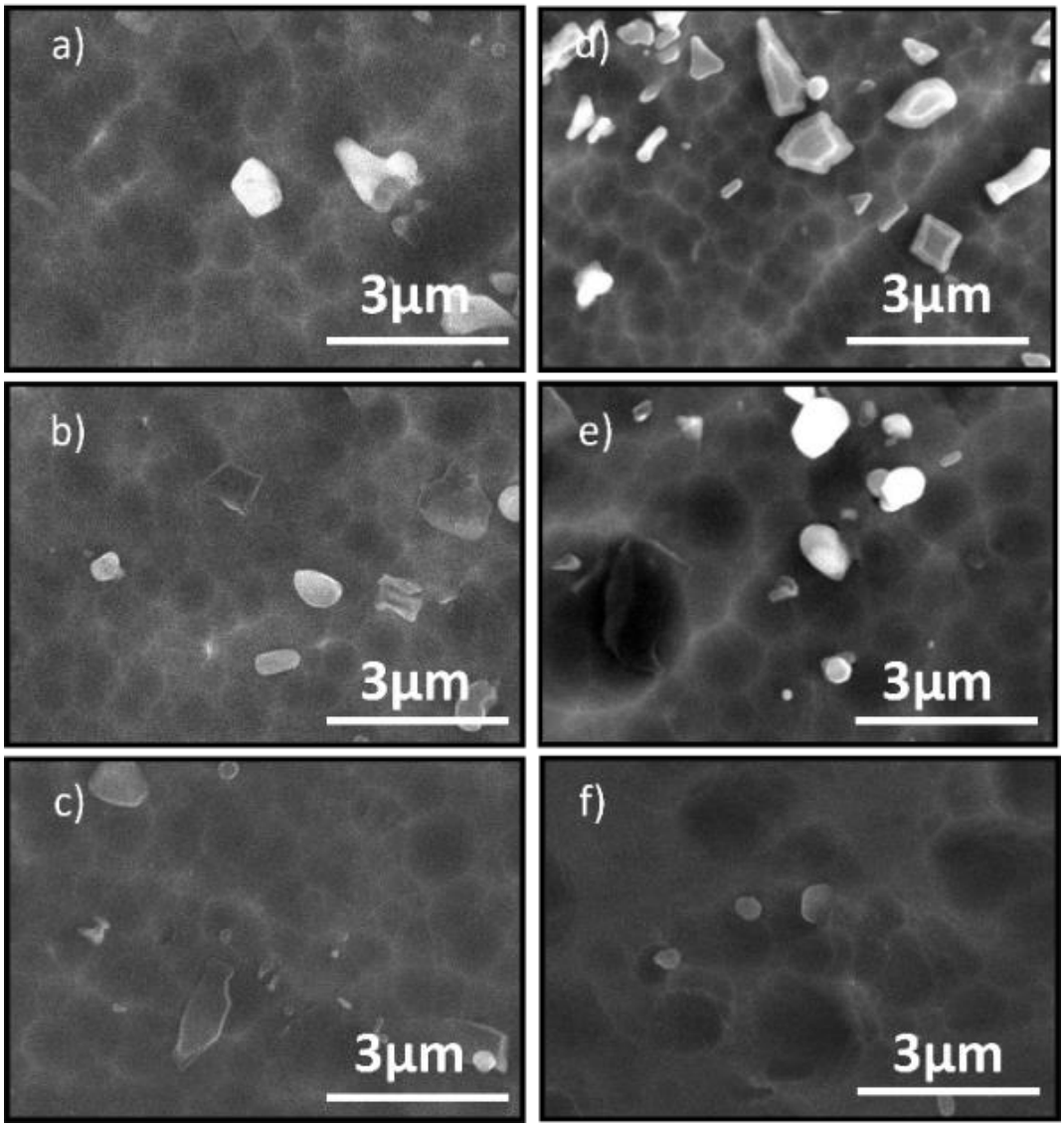

Figure 4.3 SEM images of chemically etched Al surface (30µm) etched at 20ºC for (a) 10mins (b) 15 mins (c) 20mins, 25ºC for (d) 5 mins (e) 10mins, and 30ºC for (f) 5mins

Figure 4.2 (a), demonstrates the typical structure after etching the as purchased etchant. Consequently, circular micro scale pits are formed and connected. The variation of time directly influenced the dimension of the pits. From Figure 4.2, Figure 4.3 (a,b,c) It is observed that the increment in the duration of etching, directly corresponds to the dimension of pits, and density of pits. After the certain time limit for each temperature, etching process produce some bubbles in the etchant and after which the Al foil starts dissolving. The SEM results indicates that the variation of etching temperature accelerates the etching process, while exerting the depth of etched structures which can be clearly seen by comparing the Figure 4.3 b and f. The increase in temperature influences

the depth rate in positive, as the depth of the etched pits increase with the increased temperature as shown in tilted Figure 4.4 (b), the highest depth was achieved at 5mins, 30 ºC. Which is the resultant chemical activation at high temperature [41]. The corresponding etch rate observed for 20ºC, 25ºC, 30ºC is 0.30×10^3, 0.60×10^3,1.20×10^3 Å/min [Microchemicals- Al etchant manual].

[54], also reported the same effect of time and temperature on the cavities size and aspect ratio of hierarchical microstructures on Al foil by using anodic etching technique.

The cross-sectional comparison between pristine, chemically and anodic etched foil is shown in the appendix Figure 6.1.

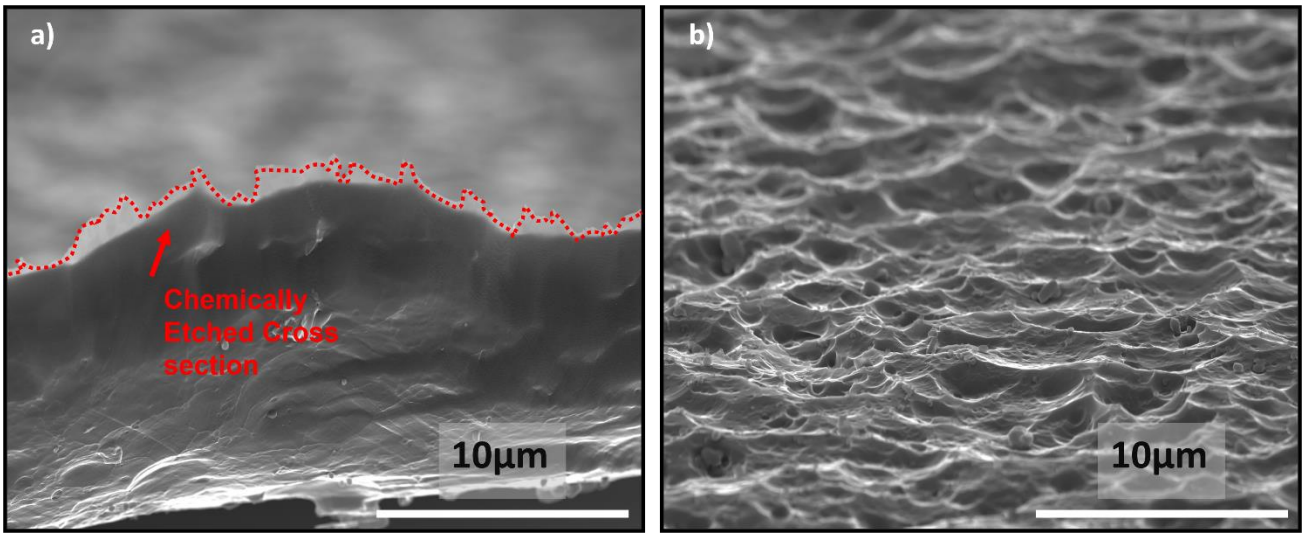

Figure 4.4 FESEM image of Al-30(5 mins,30ºC) sample (a) showing the cross-section of etched pits and oblique (25°) (b) close-up of etching showing the detail of etched morphology

Further evidence of above analysis can be proved from the measured size of etched pits using SEM are present in ***Table 2Table 3***, the above observed analysis is directly linking to the pits size here. For instance, for Al-15p foil at 20 the change in etching time varies the size of granular plates from 0.49µm to 0.67µm. Similarly, the impact of temperature can be comprehended by using Al-30p etched data from ***Table 3***, it demonstrates how the higher temperature and lower time for instance etching at 5mins, 30°C of etching achieved of almost same pit diameter of 1.1µm from 20mins, 20°C.

Table 2 : Description of effects of etching in terms of pits width (µm) on 15µm Al substrate by varying time and temperature

	5mins			10 mins			15 mins			20 mins		
	Min	max	mean	min	max	mean	min	max	mean	min	max	mean
20°C				0.33	0.67	0.49	0.304	1.026	0.58	0.50	0.87	0.67
25 °C	0.43	0.92	0.87	0.82	2.04	1.34						
30°C	0.5	1.26	1.15									

Table 3:Description of effects of etching in terms of pits width (µm) on 30µm Al substrates by varying time and temperature

	5mins			10 mins			15 mins			20 mins		
	Min	max	mean	min	max	mean	min	max	mean	min	max	mean
20°C				0.57	0.93	0.65	0.75	1.24	0.72	0.85	1.36	1.43
25 °C	0.42	1.01	0.6	0.50	1.51	1.02						
30°C	0.31	1.28	1.1									

To proceed further systematic inquire, one specimen with almost same features was chosen from each thicknesses of Al foil (Al-15, Al-30 etching sessions). Results achieved from SEM were analyzed to choose, based on the etched morphology like uniform distribution and minimal size pits.

The selected chemically etched samples and commercially purchased anodic etched foil (etching parameters and etchant are unknown)for comparison purpose is shown in Figure 4.5. It is observed from the morphology of anodic etched foil that this foil is etched by using strong acid, which attacks the rolling directions as discussed above.

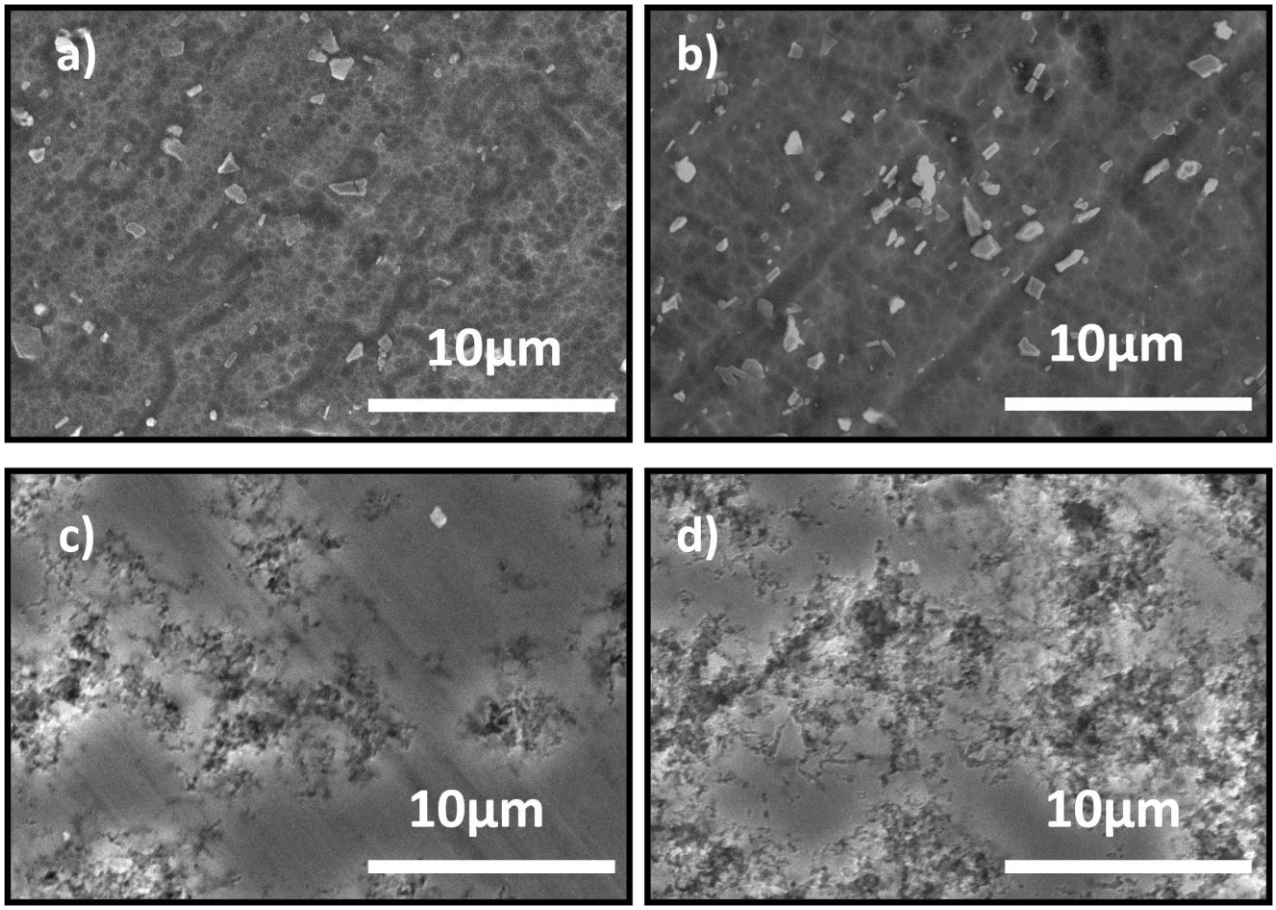

Figure 4.5 SEM Morphology of Chemically etched samples a) Al-15CE b) Al-30CE and commercially purchased Anodic etched samples c) Al-30 d) Al-70 at magnification of 10 µm

4.1.1 Statistical analysis of Al surface roughness

Since etching is the process which removes the material to roughen the surface, and surface roughness is the key parameter to evaluate the effectiveness of chemical etching process on microstructure samples. Therefore, an investigation using Atomic Force Microscopy (non-conatct mode, tip radius: <10nm, scan rate 0.4 Hz and 0.5Hz) is carried out to calculate the surface roughness of pristine, chemically etched and anodic etched samples with the scan size 10×10 μm^2.

Corresponding AFM image of Figure 4.1 is presented in fig Figure 4.6(a) and Figure 4.7(a). The analysis on pristine samples Al-15p, and Al-30p provides the valued insight into morphology. The surface map reveals the presence of continuous grooves resulting from the lamination technique, and the big peaks in the graph indicates the particles or impurities on the surface. The wider size pits on pristine foils

2D surface morphology indicate the mechanical force exerted during the manufacturing process. Hence the manufacturing of Al foil can subject to various mechanical forces, which could result in some irregularities, deformation or structures appearance on Al foil [55].

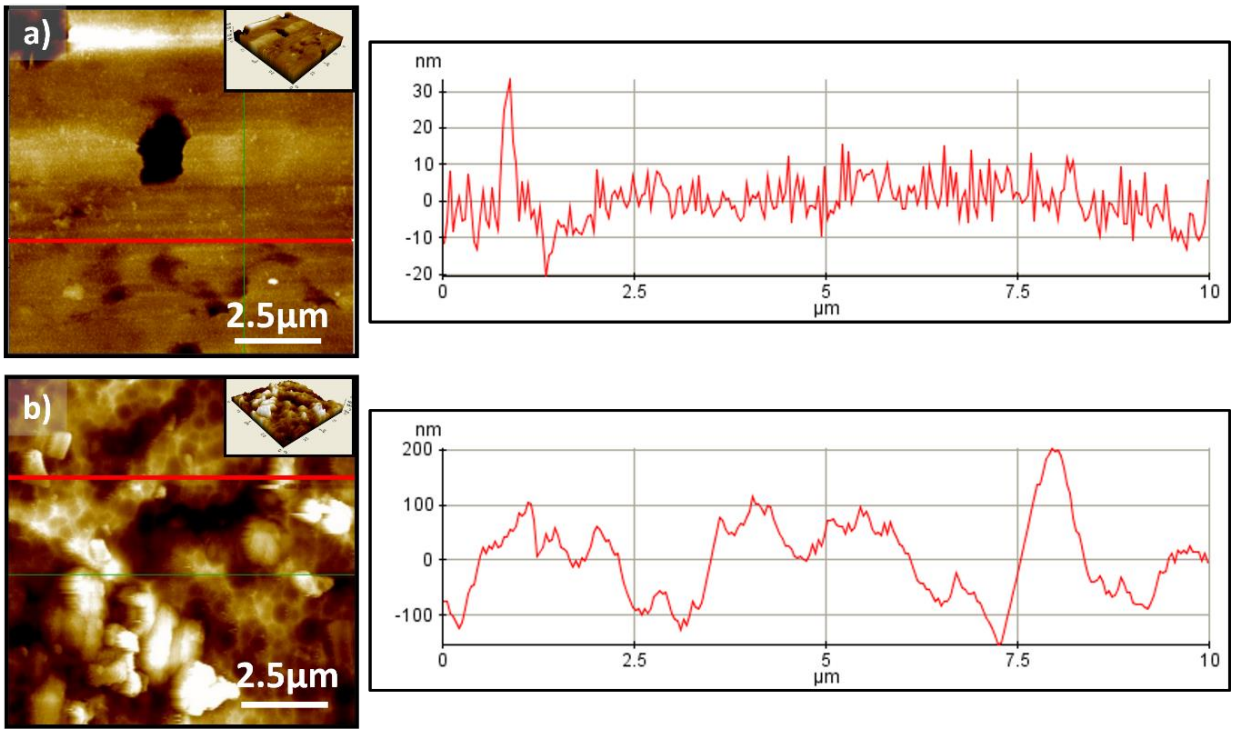

Figure 4.6 AFM images of 15µm Al substrates 3D Morphology and line profile(red) graph of (a) Al-15p (b) Al-15CE samples with the scan rate 0.4 Hz

Figure 4.6(b),Figure 4.7(b) corresponds to the after etching profile. The impact of chemical etching on etched samples quite evident from the AFM 2D profile images which depicts the higher degree of roughness on the etched surface as compared to pristine samples. The granular micro-structure of AFM mapping is quite consistent with the SEM images of etched samples present in Figure 4.5. The investigation further corroborated the findings, by revealing the presence of cavities on the surface. Referring to the Al-15 CE Figure 4.6, the cavities dimension ranging from 0.5 to 2 µm and depths of up to 180nm. Similarly, for Al-30CE, the analytical data from Figure 4.7 depicts the cavity size of up to 2µm, with the depth of the cavities ranging from 50 to 150nm. In both topography, there are some bright smuts which indicates the residuals of oxide layer, with the height of up-to 300nm.

Overall, these dimensions and depth of cavities indicate that extent of material removed during the etching process, these cavities can further affect the behaviour of Al as current collector. The results for both chemically etched samples at different parameters shows the same degree of etching on both foils despite the different time and temperature.

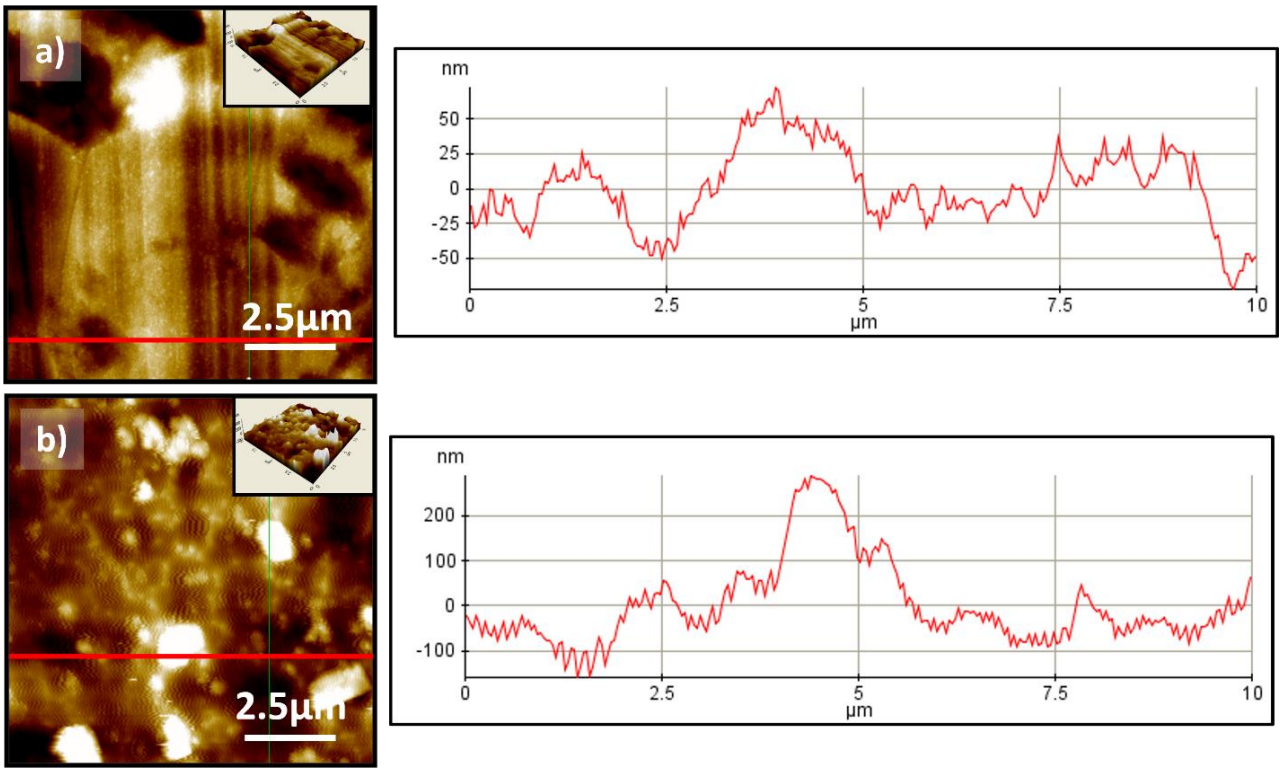

Figure 4.7 AFM images of 30µm Al substrates 3D Morphology and line profile of (a) Al-30p (b) 3D Al-30CE with the scan rate 0.4 Hz

The additional analysis on the morphology of commercially purchased anodic etched samples was performed to differentiate the features from the chemically etched samples. **Error! Reference source not found.** , illustrates the similar morphology that observed in Figure 4.5 SEM analysis. The presented figure, indicates that the morphology of anodic etched samples is different than chemically etched samples, this etching have network type cavity impacts on sample's surface. Line profile of **Error! Reference source not found.** (a) Al-30 depicts the morphology with continuous grooves and narrow cavities with depth of up-to 100 nm results in slightly roughened surface. Whereas, line profile of **Error! Reference source not found.** (b) Al-70 depicts the wide cavities of 2.5µm with the depth of these network-like-cavities ranging from 80 to 150nm.

In order to quantify the roughness of Al substrates, the roughness analysis using AFM is reported in the Table 4 .

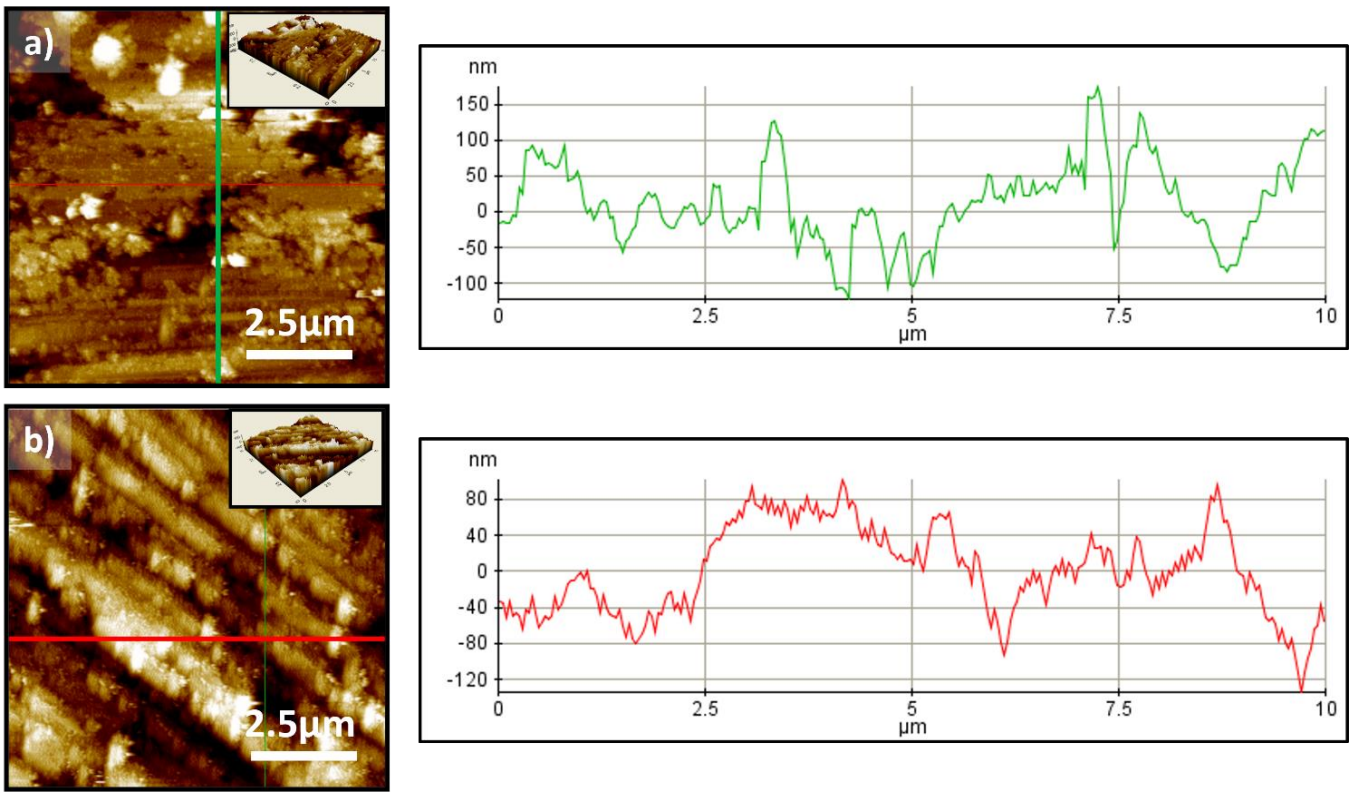

Figure 4.8: AFM images of Anodic Etched Al substrates 3D Morphology and line profile perpendicular to rolling lines (a) Al-30 (b) Al-70 with scan rate 0.5 Hz

Table 4 Roughness statistics parameters of pristine, chemically etched and commercially anodic etched foils

Specimen	**Arith.Roughness - S_a(nm)**	**RMS Roughness- S_q (nm)**
Al-15p	19	38
Al-30p	34	46
Al-15CE	69	88
Al-30CE	54	74
Al-30	36	52
Al-70	46	65

4.1.2 Electrochemical characterization of pristine and etched Al electrodes

After the etching of Al foil 3 electrode setup is used to measure the capacitance of pristine and etched foils to compare the surface gain of foils after etching. A prominent difference is seen in the capacitance of Al foil after etching, the total capacitance of both pristine foils increase by the factor of approximately 1.8.

Table 5: Capacitance measured in mF/cm^2 from CV curve using 3-electrdoe setup at 100mV/s scan rate and 0.8V potential window runs for 50cycles

Al-15p	Al-15CE	Al-30p	Al-30CE
0.14	0.25	0.13	0.22

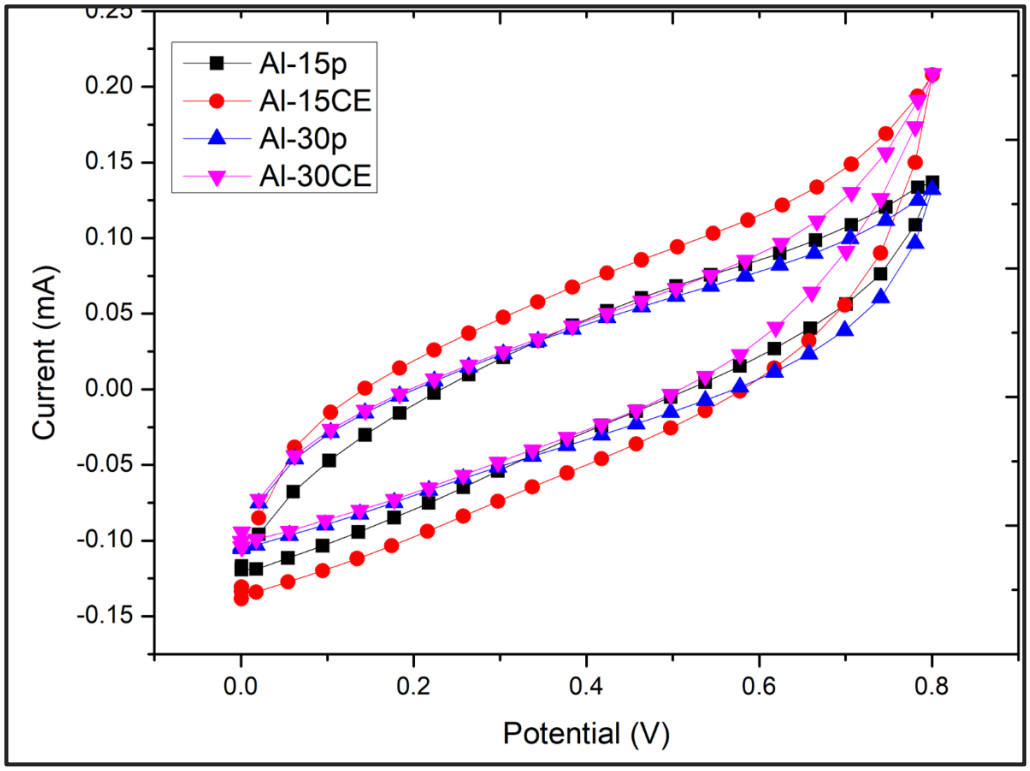

Figure 4.9: Cyclic Voltammetry measurement of pristine and chemically etched Al foils with the scanning rate 100mv/s, working potential 0.8V for 50cycles using 3-eelctrode setup

Similarly, the CV measurement on anodic etched samples Al-30 and Al-70 were performed using the same setup. The working potential window of Al-70 is different than other measured potential. For the potential of 0 to 0.8V , the resultant current shows the less gradual increase and after certain point it showed the sharp increase to 30mA as shown in [Appendix: Error! Reference source not found.]. Therefore, the working potential is narrowed to the window where it showed the gradual increase. Hence, the results prove that the oxide layer on Al-70 is thicker than Al-30, it acts as barrier which limited the electrochemical reactions between electrode surface and shifted it potential window to smaller potential window of 0.8to -0.4V.

The Al-70 electrode shows the capacitance of 1.05mF/cm^2, whereas the Al-30 shows the capacitance of 0.4mF/cm^2.

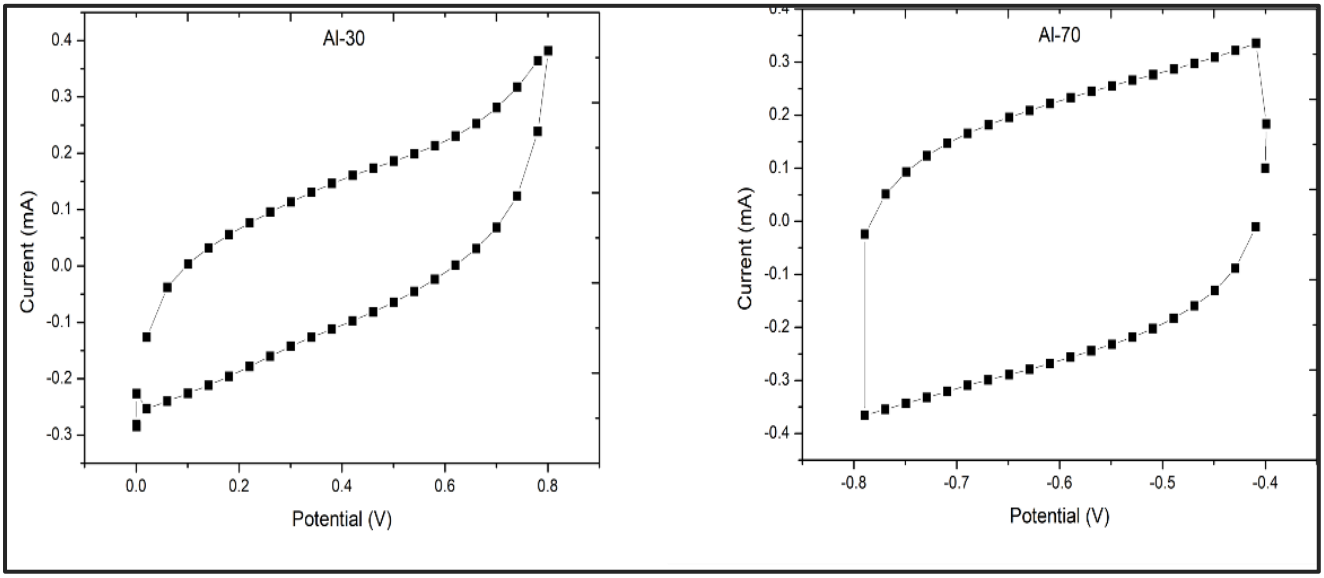

Figure 4.10: Cyclic Voltammetry measurement of commercially etched Al foils (Al-30, Al-70), with the scanning rate 100mv/s for 50cycles using 3-eelctrode setup

4.2 Effect of Morphology on Ni Deposition

The morphology of substrate have significant affect on the deposition of Ni nano particles on surface of substrate. The etching of the pristine Al substrate increases the surface area of foil. As the consequence of this surface gain, the deposition of Ni nanoparticles on per unit area directs to the reduction in size of Ni nanoparticle as compare to the Ni deposited on smooth surface.

The chemical etching of Al foil results in the granular-plate like structure which provides more nucleation site for Ni to deposit as compared to a smooth surface, resulting in the higher density of Ni nano particles, but in smaller individual size. Figure 4.11, demonstrates the deposition of 10nm Ni on both chemically and anodically etched foils. The substrate morphology has significantly influenced the distribution, size and shape of Ni nano-particles. Since the deposition size of nanoparticles is inversely proportional to the surface area of substrate. From above capacitance results it can be seen that the surface gain of anodic etched foil is approximately double to the surface gain of chemically etched samples. Therefore in Figure 4.11(a), the Ni particles of round shape of about ~8nm size are less scattered and more uniformly distributed on the surface of substrate. However, since the surface area of anodic etched foil is more rougher and based on deep network like cavities, the Ni nanoparticles of less than 7nm size are dispersed and distributed non-uniformly on the porous nucleation sites [56]. The deposition of Ni on etched surfaces results in the growth of perpendicular CNTs to the surface which can further provide the chance of getting cross-linked CNTs.

It can be summarize in this way that the etching of Al leads to provide more nucleation sites of Ni and the surface area of etched surface is efficiently divided among higher number of Nanoparticles, influencing the size of nanoparticles.

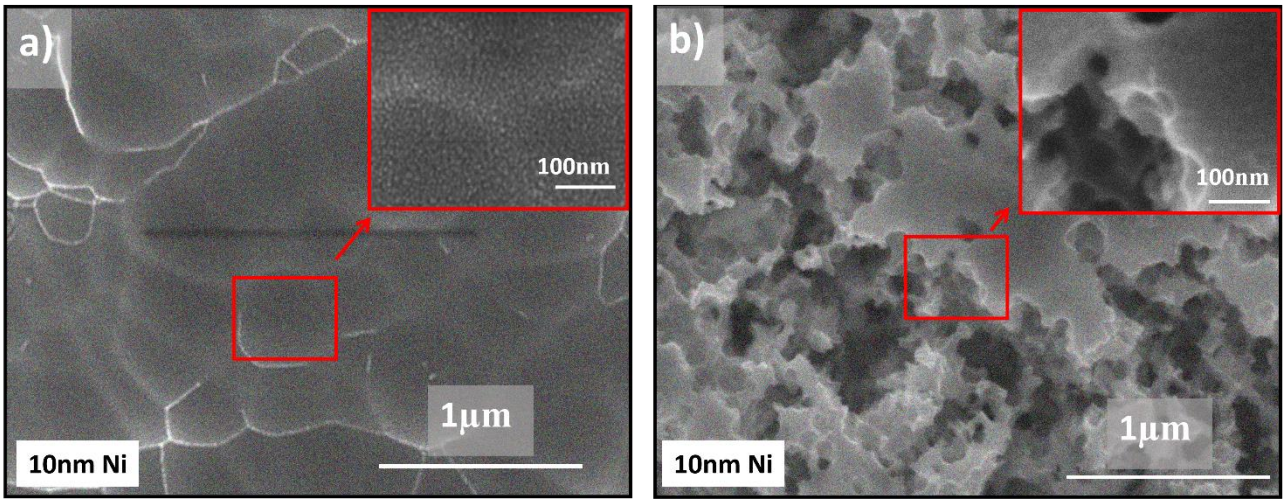

Figure 4.11 FESEM images of Ni morphology on (a) Al-30CE (b) Al-30 with the magnified image

4.3 Effect of Morphology on CNTs Growth

The effect of substrate's Morphology is investigated by growing CNTs using CVD process. The CNTs were grown on pristine Al foils, Al-15p, Al-30p, chemically etched samples Al-15CE, Al-30CE and commercially etched samples Al-30, Al 70. As shown in Figure 4.12, the growth of CNTs follow the morphology of substrate and deposited Ni morphology. Form Figure 4.11(a), we conclude that the deposition of Ni nanoparticles on chemically etched samples was more evident and continuous as compared to the anodic etched foil because of the morphology difference. Since the pristine foils have smooth morphology which is proved in previous section, the growth on these sample could be ~10nm and after heat treatment the size of Ni nano particle increases [48]. In Figure 4.12 (a) (d), shoes the growth of CNTs with some bright particles that could be Ni catalyst causing tip growth due to the weak bonding/interaction between the catalyst and substrate as mentioned in [57]. Moreover, the diameter of CNTs varies from 50 to 130nm. Whereas on etched samples Figure 4.12 (b) (c), CNTs of up-to 80nm are measured with some thick CNTs of up to 100nm on surface and diameter of CNTs in pits get thinner up-to 40nm. Overall, the synthesis of pure CNTs is achieved on all the substrates. Figure 4.12 (e),(f), the CNTs grown on Al-30 and Al-70 morphology provides more deep nucleation sites, hence the CNTs on these sample are more in depth. And the diameter in this case gets thinner to 30nm due to size of Ni nanoparticle.

It can be summarize as, the etching of Al foil increases the surface area of the substrate. As a consequence, it increased the deposition of Ni particles on the substrate, subsequently causing the higher degree of CNTs growth. The diameter of CNTs depend on the size of Ni nanoparticles. Therefore, on anodic etched samples more thinner diameter CNTs are observed as compared to the chemically etched samples.

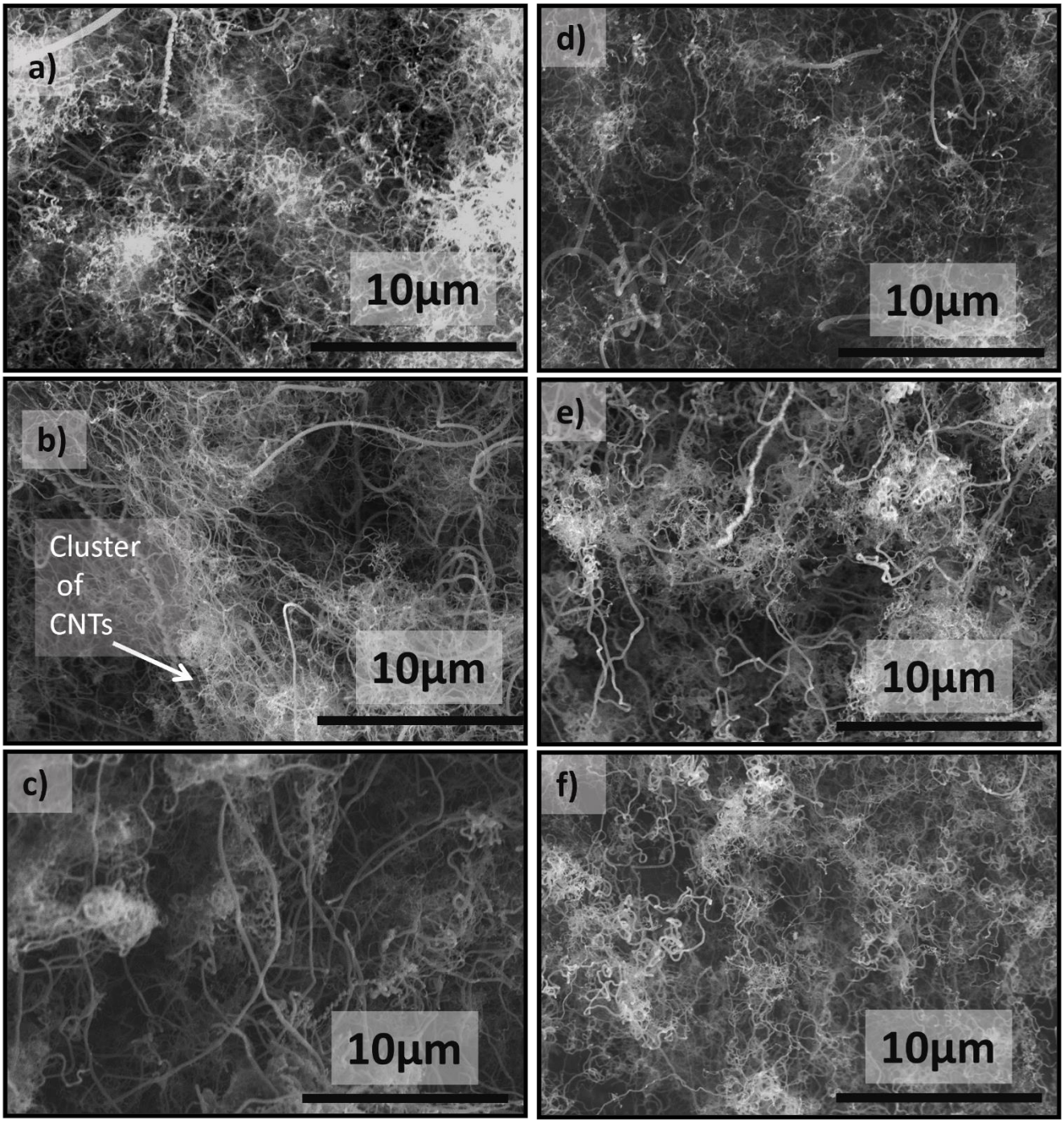

Figure 4.12 SEM images of iCL -CNTs grown on (a) Al-15p (b)Al-15CE (c)Al-30CE (d)Al-30p (e)Al-30p (f) Al-70

Based on the CNTs adhesion comparison between the CNTs grown on pristine and chemically etched Al foils, as it can be shown in that the CNTs grown on pristine foil had poor adhesion to the surface and were easy to peel off as compared to the etched samples. The CNTs grown on etched samples exhibited the firm adhesion to the surface and they were grown inside the pits which make them

difficult to peel off easily. This suggests that the etching of smooth Al foil can enhance the adhesion property by providing more surface area and creating strong bonding. This behavior was also observed in [58].

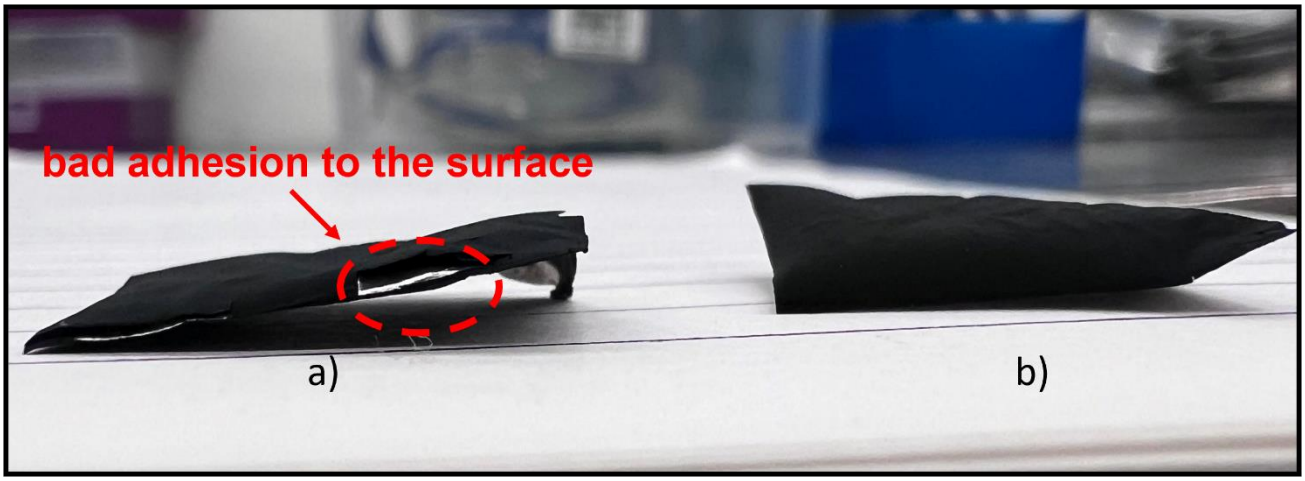

Figure 4.13 Illustration of adhesiveness of CNTs grown on a) Al-15p b) Al-15CE

The mass of CNTs obtained using the equation given in appendix

Table 6 Mass of CNTs measured on pristine, chemically and Anodic etched foils in mg/cm^2

Al-15p	Al-15CE	Al-30p	Al-30CE	Al-30	Al-70
2.3	2.4	2.3	2.2	1.8	2.4

4.3.1 Electrochemical characterization of CNTs based electrodes

The CNTs grown on modified Al substrates are further characterized by electrochemical characterization. The voltage scan of 100mV/s is applied between the working electrode and graphite counter electrode, with the potential window of 0-0.8V for CV measurements as shown in Figure 4.14. CV curves for each electrode is analyzed and the specific capacitance is measured by using eq 3.4 with the help of Origin 8.5 software.

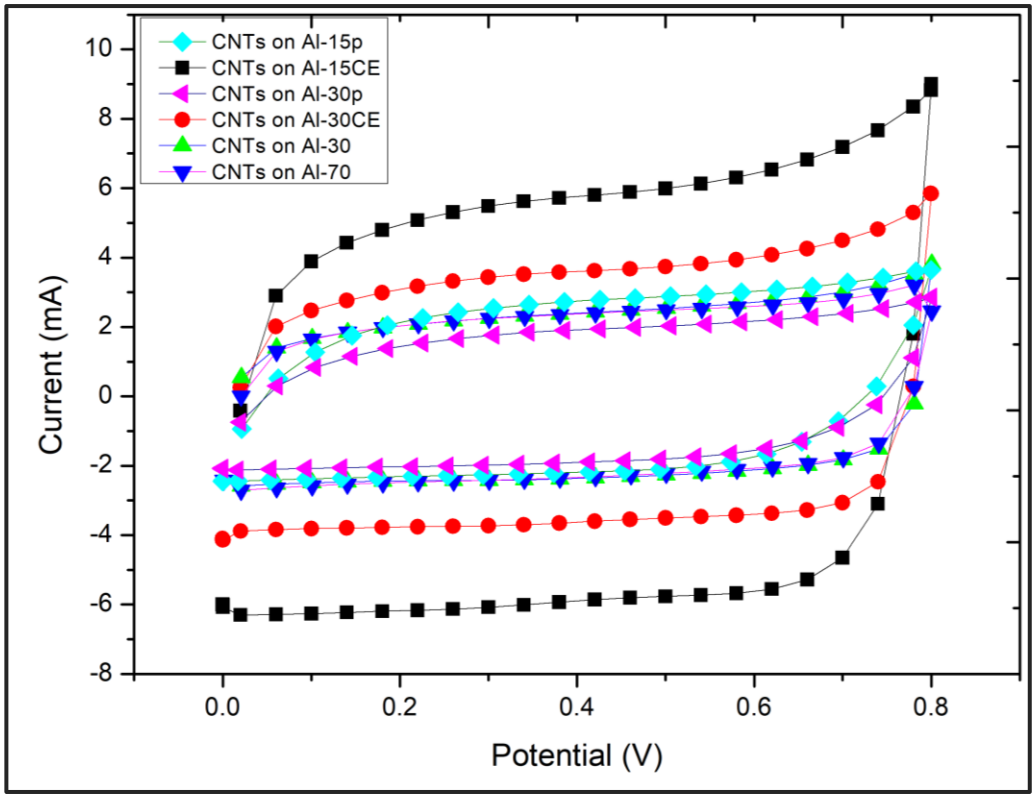

Figure 4.14 Cyclic Voltammetry (CV) of CNTs based electrodes at 100mv/s scan rate and potential window of 0.8V

Table 7: Capacitance measured using 3 electrode setup by CV measure at 100mV/s for CNTs grown on Al-15p, Al-15CE, Al-30p, Al-30CE, Al-30 and Al-70 in mF/cm^2

Al-15p	Al-15CE	Al-30p	Al-30CE	Al-30	Al-70
17	26.50	14.43	24	21.27	21.00

CNTs grown on chemically etched Al substrates shows the high current response in CV curve. Upon applying the voltage across the terminals the current flowing through the capacitor changes right after an initial transient response. The different gradual changes in currents for each electrode shows that the capacitance depends on the area/morphology of electrode. After a certain point the current in graph increases sharply, viewing the faradic charge transfer by the commence of redox reactions [59]. The rise in current density after etching, shows the increase in capacitance of CNTs grown on Al-15CE and Al-30CE samples by the factor of ~1.6. Corresponds to the increase in surface area. The CNTs grown on anodic etched samples shows almost same capacitance of 21.27mF/cm^2, with no prominent

difference. Anodic etched samples upon comparing with chemical etched sample shows the capacitance that is slightly lower than chemically etched samples. The chemical etching causes more uniform kind of structure after etching whereas the anodic etched samples causes more deep but less uniform pores.

Since the capacitance of electrode is determined by the surface area available for charge storage in eq 3.4. The above capacitance values prove that the etching of Al foil increases the surface area of sample which further provide more nucleation sites for the growth of CNTs to store more charge.

5 Conclusion and Future Work

The above study concludes that, the optimization of Al substrate is successfully implemented by using chemical etching for the growth of CNTs for high energy density of supercapacitors by improving the specific capacitance of chemically etched electrodes. Since, the proposed study improves the specific area of the current collector which further (i) provides more nucleation sites for the deposition of Ni nanoparticles and it was quite evident from the FESEM analysis (ii) that it further helps in the synthesis of higher degree of CNTs (iii) this increase in CNTs provides more surface area for an electrode to store charge , and all these results directly link to the increase in the specific capacitance of electrode.

The research study employed the chemical etching method (ANPE, Microchemical) and a systematic comparative study is made with commercially bought anodic etched foil. First part of research using SEM for morphology analysis, reveals the resultant granular-plate like structure from chemical etched samples Al-15CE, Al-30CE, which is different than commercially purchased anodic etched foil due to the method and the etchant behaviour. The dimension of these pits increase by changing the time which ranges from 0.3µm to 2µm and the temperature impacted the etching rate and depth of pits. Characterization of AFM proves the average roughness of etched samples increase by the factor of ~2 from pristine samples. Moreover, the capacitance testing using three-electrode setup confirms the increment in surface area by showing the capacitance increased by factor of ~1.8.

The second part of research carries out the effect of morphology of 10nm Ni deposition using sputtering technique on chemically etched samples and anodic etched samples using FESEM. The resultant morphology analysis reveals deposition of less scattered Ni-nanoparticles on the small and uniform etched pits of chemically etched samples, whereas, the morphology of anodic etched samples is based of large network like cavities which makes it hard to observe the Ni nanoparticles on surface.

Finally, the effect of morphology is confirmed on the synthesis of CNTs using chemical Vapor deposition procedure with the gas composition of (Ar: H_2: C_2H_2 40:100:20) with synthesis time of 15 mins on pristine foils Al-15p, Al-30p chemically etched samples Al-15CE, Al-30CE and anodic etched samples Al-30 , Al-70. The result confirms that the etching of Al foil not just increases the surface area but also improves the adhesion of CNTs to the current collector. The electrochemical performance of CNTs grown on chemically etched substrates Al-15CE(26.50 mF/cm^2), Al-30CE(24 mF/cm^2) is found to

be almost similar to anodic etched commercially purchased etched samples Al-30(21.27mF/cm^2). Al-70(21 mF/cm^2) .

Overall, the proposed study highlighted the effect of morphology on CNTs growth and potential of low cost, easy to handle and highly efficient chemical etching method for the optimization of Al to achieve the results that improves the electrochemical performance of supercapacitor and also produces the comparable results to commercially purchased anodic etched foils.

Though more work is required to investigate the more optimal solution. Following tasks in the future can be performed to investigate the better optimal solution:

1. Scalability of this etching technique may encounters some challenges and modifications that can be addressed in future studies
2. A small optimization of Ni catalyst deposition and CVD recipe on the chemically etched samples can improve the mass loading and capacitance of electrodes
3. Similar comparative study can be performed on other etched samples with different parameters to find the optimal substrate among all
4. The process optimization can also be performed by employing another etching parameter, etchant dilution (concentration of etchant) which will certainly show effect on etching behaviour and rate of etching
5. Exploration of more etchants or etching techniques like plasma enhanced, selective material etching by masking substrate and electrochemical etching could improve the results with unique properties
6. Same study could be conducted on other common metallic substrates for growth of CNTs for supercapacitors e.g. Copper (Cu), and Nickel (Ni) to examine their potential for growing CNTs

References

[1] M. Dhimish and A. M. Tyrrell, “Power loss and hotspot analysis for photovoltaic modules affected by potential induced degradation,” *Npj Mater. Degrad.*, vol. 6, no. 1, p. 11, Feb. 2022, doi: 10.1038/s41529-022-00221-9.

[2] H. Gong and J. Sun, “Phosphorus-based nanomaterials for lithium-ion battery anode,” in *Encyclopedia of Nanomaterials*, Elsevier, 2023, pp. 533–549. doi: 10.1016/B978-0-12-822425-0.00086-5.

[3] Q. Cheng, J. Duan, Q. Zhang, and L. Jiang, “Learning from Nature: Constructing Integrated Graphene-Based Artificial Nacre,” *ACS Nano*, vol. 9, no. 3, pp. 2231–2234, Mar. 2015, doi: 10.1021/acsnano.5b01126.

[4] Department of Electrical and Electronics Engineering, SRM University, Kattankulathur, India 603203. and Z. S. Iro, “A Brief Review on Electrode Materials for Supercapacitor,” *Int. J. Electrochem. Sci.*, pp. 10628–10643, Dec. 2016, doi: 10.20964/2016.12.50.

[5] Y.-G. Lee *et al.*, “High-energy long-cycling all-solid-state lithium metal batteries enabled by silver–carbon composite anodes,” *Nat. Energy*, vol. 5, no. 4, pp. 299–308, Mar. 2020, doi: 10.1038/s41560-020-0575-z.

[6] M. F. El-Kady, Y. Shao, and R. B. Kaner, “Graphene for batteries, supercapacitors and beyond,” *Nat. Rev. Mater.*, vol. 1, no. 7, p. 16033, May 2016, doi: 10.1038/natrevmats.2016.33.

[7] A. Szabó *et al.*, “Influence of synthesis parameters on CCVD growth of vertically aligned carbon nanotubes over aluminum substrate,” *Sci. Rep.*, vol. 7, no. 1, p. 9557, Aug. 2017, doi: 10.1038/s41598-017-10055-0.

[8] W. Thongsuwan, W. Sroila, T. Kumpika, E. Kantarak, and P. Singjai, “Antireflective, photocatalytic, and superhydrophilic coating prepared by facile sparking process for photovoltaic panels,” *Sci. Rep.*, vol. 12, no. 1, p. 1675, Jan. 2022, doi: 10.1038/s41598-022-05733-7.

[9] A. Abdisattar *et al.*, “Recent advances and challenges of current collectors for supercapacitors,” *Electrochem. Commun.*, vol. 142, p. 107373, Sep. 2022, doi: 10.1016/j.elecom.2022.107373.

[10] P. L. Taberna, S. Mitra, P. Poizot, P. Simon, and J.-M. Tarascon, “High rate capabilities Fe3O4-based Cu nano-architectured electrodes for lithium-ion battery applications,” *Nat. Mater.*, vol. 5, no. 7, pp. 567–573, Jul. 2006, doi: 10.1038/nmat1672.

[11] X. Sedao *et al.*, “Growth Twinning and Generation of High-Frequency Surface Nanostructures in Ultrafast Laser-Induced Transient Melting and Resolidification,” *ACS Nano*, vol. 10, no. 7, pp. 6995–7007, Jul. 2016, doi: 10.1021/acsnano.6b02970.

[12] N. A. Salleh, S. Kheawhom, and A. A. Mohamad, “Characterizations of nickel mesh and nickel foam current collectors for supercapacitor application,” *Arab. J. Chem.*, vol. 13, no. 8, pp. 6838–6846, Aug. 2020, doi: 10.1016/j.arabjc.2020.06.036.

[13] R. Wang *et al.*, “Carbon black/graphene-modified aluminum foil cathode current collectors for lithium ion batteries with enhanced electrochemical performances,” *J. Electroanal. Chem.*, vol. 833, pp. 63–69, Jan. 2019, doi: 10.1016/j.jelechem.2018.11.007.

[14] Y. Zhang, C. Sun, and Z. Tang, “High specific capacitance and high energy density supercapacitor electrodes enabled by porous carbon with multilevel pores and self-doped heteroatoms derived from Chinese date,” *Diam. Relat. Mater.*, vol. 97, p. 107455, Aug. 2019, doi: 10.1016/j.diamond.2019.107455.

[15] A. K. Samantara and S. Ratha, “Historical Background and Present Status of the Supercapacitors,” in *Materials Development for Active/Passive Components of a Supercapacitor*, in SpringerBriefs in Materials. Singapore: Springer Singapore, 2018, pp. 9–10. doi: 10.1007/978-981-10-7263-5_2.
[16] S. Banerjee *et al.*, “Capacitor to Supercapacitor,” in *Handbook of Nanocomposite Supercapacitor Materials I*, K. K. Kar, Ed., in Springer Series in Materials Science, vol. 300. Cham: Springer International Publishing, 2020, pp. 53–89. doi: 10.1007/978-3-030-43009-2_2.
[17] J. Castro-Gutiérrez, A. Celzard, and V. Fierro, “Energy Storage in Supercapacitors: Focus on Tannin-Derived Carbon Electrodes,” *Front. Mater.*, vol. 7, p. 217, Jul. 2020, doi: 10.3389/fmats.2020.00217.
[18] M. V. Kiamahalleh, S. H. S. Zein, G. Najafpour, S. A. Sata, and S. Buniran, “MULTIWALLED CARBON NANOTUBES BASED NANOCOMPOSITES FOR SUPERCAPACITORS: A REVIEW OF ELECTRODE MATERIALS,” *Nano*, vol. 07, no. 02, p. 1230002, Apr. 2012, doi: 10.1142/S1793292012300022.
[19] J. Xie, P. Yang, Y. Wang, T. Qi, Y. Lei, and C. M. Li, “Puzzles and confusions in supercapacitor and battery: Theory and solutions,” *J. Power Sources*, vol. 401, pp. 213–223, Oct. 2018, doi: 10.1016/j.jpowsour.2018.08.090.
[20] R. Nigam, P. Sinha, and K. K. Kar, “Introduction to Supercapacitors,” in *Handbook of Nanocomposite Supercapacitor Materials III*, K. K. Kar, Ed., in Springer Series in Materials Science, vol. 313. Cham: Springer International Publishing, 2021, pp. 1–38. doi: 10.1007/978-3-030-68364-1_1.
[21] B. E. Conway, “Transition from ‘Supercapacitor’ to ‘Battery’ Behavior in Electrochemical Energy Storage,” *J. Electrochem. Soc.*, vol. 138, no. 6, pp. 1539–1548, Jun. 1991, doi: 10.1149/1.2085829.
[22] K. Yu *et al.*, “Hierarchical vertically oriented graphene as a catalytic counter electrode in dye-sensitized solar cells,” *J Mater Chem A*, vol. 1, no. 2, pp. 188–193, 2013, doi: 10.1039/C2TA00380E.
[23] P. Sinha, S. Banerjee, and K. K. Kar, “Characteristics of Activated Carbon,” in *Handbook of Nanocomposite Supercapacitor Materials I*, K. K. Kar, Ed., in Springer Series in Materials Science, vol. 300. Cham: Springer International Publishing, 2020, pp. 125–154. doi: 10.1007/978-3-030-43009-2_4.
[24] B. De *et al.*, “Transition Metal Oxide/Electronically Conducting Polymer Composites as Electrode Materials for Supercapacitors,” in *Handbook of Nanocomposite Supercapacitor Materials II*, K. K. Kar, Ed., in Springer Series in Materials Science, vol. 302. Cham: Springer International Publishing, 2020, pp. 353–385. doi: 10.1007/978-3-030-52359-6_14.
[25] A. Abdulhameed, N. Z. A. Wahab, M. N. Mohtar, M. N. Hamidon, S. Shafie, and I. A. Halin, “Methods and Applications of Electrical Conductivity Enhancement of Materials Using Carbon Nanotubes,” *J. Electron. Mater.*, vol. 50, no. 6, pp. 3207–3221, Jun. 2021, doi: 10.1007/s11664-021-08928-2.
[26] J. K. H. Wong, S. T. Kok, and S. Y. Wong, “Fibers, Geopolymers, Nano and Alkali-Activated Materials for Deep Soil Mix Binders,” *Civ. Eng. J.*, vol. 6, no. 4, pp. 830–847, Apr. 2020, doi: 10.28991/cej-2020-03091511.
[27] O. Zaytseva and G. Neumann, “Carbon nanomaterials: production, impact on plant development, agricultural and environmental applications,” *Chem. Biol. Technol. Agric.*, vol. 3, no. 1, p. 17, Dec. 2016, doi: 10.1186/s40538-016-0070-8.
[28] K. D. Verma, P. Sinha, S. Banerjee, and K. K. Kar, “Characteristics of Current Collector Materials for Supercapacitors,” in *Handbook of Nanocomposite Supercapacitor Materials I*, K. K. Kar, Ed., in Springer Series in Materials Science, vol. 300. Cham: Springer International Publishing, 2020, pp. 327–340. doi: 10.1007/978-3-030-43009-2_12.

[29] H. Trivedi, K. D. Verma, P. Sinha, and K. K. Kar, “Current Collector Material Selection for Supercapacitors,” in *Handbook of Nanocomposite Supercapacitor Materials III*, K. K. Kar, Ed., in Springer Series in Materials Science, vol. 313. Cham: Springer International Publishing, 2021, pp. 271–311. doi: 10.1007/978-3-030-68364-1_8.

[30] K. D. Verma, P. Sinha, S. Banerjee, and K. K. Kar, “Characteristics of Current Collector Materials for Supercapacitors,” in *Handbook of Nanocomposite Supercapacitor Materials I*, K. K. Kar, Ed., in Springer Series in Materials Science, vol. 300. Cham: Springer International Publishing, 2020, pp. 327–340. doi: 10.1007/978-3-030-43009-2_12.

[31] A. Tanwilaisiri, Y. Xu, D. Harrison, J. Fyson, and M. Arier, “A Study of Metal Free Supercapacitors Using 3D Printing,” *Int. J. Precis. Eng. Manuf.*, vol. 19, no. 7, pp. 1071–1079, Jul. 2018, doi: 10.1007/s12541-018-0127-7.

[32] P. Luo and L. Huang, “Carbon Paper as Current Collectors in Graphene Hydrogel Electrodes for High-Performance Supercapacitors,” *Nanomaterials*, vol. 10, no. 4, p. 746, Apr. 2020, doi: 10.3390/nano10040746.

[33] M. D. S. Klem, R. M. Morais, R. J. G. Rubira, and N. Alves, “Paper-based supercapacitor with screen-printed poly (3, 4-ethylene dioxythiophene)-poly (styrene sulfonate)/multiwall carbon nanotube films actuating both as electrodes and current collectors,” *Thin Solid Films*, vol. 669, pp. 96–102, Jan. 2019, doi: 10.1016/j.tsf.2018.10.029.

[34] S. A. Baskakov *et al.*, “Fabrication of current collector using a composite of polylactic acid and carbon nano-material for metal-free supercapacitors with graphene oxide separators and microwave exfoliated graphite oxide electrodes,” *Electrochimica Acta*, vol. 260, pp. 557–563, Jan. 2018, doi: 10.1016/j.electacta.2017.12.102.

[35] E.-C. Cho *et al.*, “PEDOT-modified laser-scribed graphene films as bginder– and metallic current collector–free electrodes for large-sized supercapacitors,” *Appl. Surf. Sci.*, vol. 518, p. 146193, Jul. 2020, doi: 10.1016/j.apsusc.2020.146193.

[36] S. A. Kazaryan, S. N. Razumov, S. V. Litvinenko, G. G. Kharisov, and V. I. Kogan, “Mathematical Model of Heterogeneous Electrochemical Capacitors and Calculation of Their Parameters,” *J. Electrochem. Soc.*, vol. 153, no. 9, p. A1655, 2006, doi: 10.1149/1.2212057.

[37] S. Dörfler *et al.*, “High power supercap electrodes based on vertical aligned carbon nanotubes on aluminum,” *J. Power Sources*, vol. 227, pp. 218–228, Apr. 2013, doi: 10.1016/j.jpowsour.2012.11.068.

[38] B. Panda, I. Dwivedi, K. Priya, P. B. Karandikar, and P. S. Mandake, “Analysis of aqueous supercapacitor with various current collectors, binders and adhesives,” in *2016 Biennial International Conference on Power and Energy Systems: Towards Sustainable Energy (PESTSE)*, Bangalore: IEEE, Jan. 2016, pp. 1–6. doi: 10.1109/PESTSE.2016.7516457.

[39] P. H. Jampani, A. Manivannan, and P. N. Kumta, “Advancing the Supercapacitor Materials and Technology Frontier for Improving Power Quality,” *Electrochem. Soc. Interface*, vol. 19, no. 3, pp. 57–62, 2010, doi: 10.1149/2.F07103if.

[40] B. Bhushan, Ed., “Wet Chemical Processing,” in *Encyclopedia of Nanotechnology*, Dordrecht: Springer Netherlands, 2016, pp. 4380–4380. doi: 10.1007/978-94-017-9780-1_101174.

[41] O. Çakır, “Chemical etching of aluminium,” *J. Mater. Process. Technol.*, vol. 199, no. 1–3, pp. 337–340, Apr. 2008, doi: 10.1016/j.jmatprotec.2007.08.012.

[42] A. Khaskhoussi, L. Calabrese, S. Patané, and E. Proverbio, “Effect of Chemical Surface Texturing on the Superhydrophobic Behavior of Micro–Nano-Roughened AA6082 Surfaces,” *Materials*, vol. 14, no. 23, p. 7161, Nov. 2021, doi: 10.3390/ma14237161.

[43] R. Xiao, K. Yan, J. Yan, and J. Wang, “Electrochemical etching model in aluminum foil for capacitor,” *Corros. Sci.*, vol. 50, no. 6, pp. 1576–1583, Jun. 2008, doi: 10.1016/j.corsci.2008.02.017.
[44] D. Yang and A. Laforgue, “Laser Surface Roughening of Aluminum Foils for Supercapacitor Current Collectors,” *J. Electrochem. Soc.*, vol. 166, no. 12, pp. A2503–A2512, 2019, doi: 10.1149/2.0601912jes.
[45] M. A. Ermakova, D. Y. Ermakov, A. L. Chuvilin, and G. G. Kuvshinov, “Decomposition of Methane over Iron Catalysts at the Range of Moderate Temperatures: The Influence of Structure of the Catalytic Systems and the Reaction Conditions on the Yield of Carbon and Morphology of Carbon Filaments,” *J. Catal.*, vol. 201, no. 2, pp. 183–197, Jul. 2001, doi: 10.1006/jcat.2001.3243.
[46] L. Yuan, K. Saito, W. Hu, and Z. Chen, “Ethylene flame synthesis of well-aligned multi-walled carbon nanotubes,” *Chem. Phys. Lett.*, vol. 346, no. 1–2, pp. 23–28, Sep. 2001, doi: 10.1016/S0009-2614(01)00959-9.
[47] M. V. Twigg, *Catalyst Handbook*, 2nd ed. Routledge, 2018. doi: 10.1201/9781315138862.
[48] Q. Wei *et al.*, “Ni Nanoparticles supported on N-doped carbon nanotubes for efficient hydrogenation of C5 hydrocarbon resins under mild conditions,” *Microporous Mesoporous Mater.*, vol. 333, p. 111727, Mar. 2022, doi: 10.1016/j.micromeso.2022.111727.
[49] G. Atthipalli, R. Epur, P. N. Kumta, M. Yang, J.-K. Lee, and J. L. Gray, “Nickel Catalyst-Assisted Vertical Growth of Dense Carbon Nanotube Forests on Bulk Copper,” *J. Phys. Chem. C*, vol. 115, no. 9, pp. 3534–3538, Mar. 2011, doi: 10.1021/jp108624n.
[50] *Design, Fabrication, and Characterization of Multifunctional Nanomaterials*. Elsevier, 2022. doi: 10.1016/C2019-0-00948-X.
[51] K.-Y. Lee, W.-M. Yeoh, S.-P. Chai, S. Ichikawa, and A. R. Mohamed, “The role of water vapor in carbon nanotube formation via water-assisted chemical vapor deposition of methane,” *J. Ind. Eng. Chem.*, vol. 18, no. 4, pp. 1504–1511, Jul. 2012, doi: 10.1016/j.jiec.2012.02.015.
[52] B. Voigtländer, *Atomic Force Microscopy*. in NanoScience and Technology. Cham: Springer International Publishing, 2019. doi: 10.1007/978-3-030-13654-3.
[53] Y. Zhang, J. Wu, X. Yu, and H. Wu, “Low-cost one-step fabrication of superhydrophobic surface on Al alloy,” *Appl. Surf. Sci.*, vol. 257, no. 18, pp. 7928–7931, Jul. 2011, doi: 10.1016/j.apsusc.2011.03.096.
[54] J. Scherer, O. m. Magnussen, T. Ebel, and R. J. Behm, “Initial stages of the anodic etching of aluminum foils studied by atomic force microscopy,” *Corros. Sci.*, vol. 41, no. 1, pp. 35–55, Jan. 1999, doi: 10.1016/S0010-938X(98)00128-0.
[55] R. Leach, “Surface Topography Characterisation,” in *Fundamental Principles of Engineering Nanometrology*, Elsevier, 2014, pp. 241–294. doi: 10.1016/B978-1-4557-7753-2.00008-6.
[56] Y. C. Choi *et al.*, “Effect of surface morphology of Ni thin film on the growth of aligned carbon nanotubes by microwave plasma-enhanced chemical vapor deposition,” *J. Appl. Phys.*, vol. 88, no. 8, p. 4898, 2000, doi: 10.1063/1.1314614.
[57] R. Purohit, K. Purohit, S. Rana, R. S. Rana, and V. Patel, “Carbon Nanotubes and Their Growth Methods,” *Procedia Mater. Sci.*, vol. 6, pp. 716–728, 2014, doi: 10.1016/j.mspro.2014.07.088.
[58] J. Du *et al.*, “High Peel Strength and Flexible Aligned Carbon Nanotubes/Etched Al Foil Composites with Boosted Supercapacitor and Thermal Dissipation Performances,” *Ind. Eng. Chem. Res.*, vol. 59, no. 4, pp. 1549–1558, Jan. 2020, doi: 10.1021/acs.iecr.9b05646.
[59] B. E. . Conway, *Electrochemical Supercapacitors: Scientific Fundamentals and Technological Applications*. Cham: Springer International Publishing.

6 Appendix

$$Mass\ Loading\ of\ CNTs = \frac{mass\ of\ CNTs\ (mg)}{area\ of\ specimen\ (cm^2)}\ 6.1$$

Table 8 Description of experimental parameters (time and temperature) variation for etching Al

Sample	Temperature (°C)	Time (mins)
Al-15p	20	5,10, 15, 20
	25	5,10
	30	5
Al-30p	20	10,15,20,25,30
	25	5, 10, 15, 20
	30	2,4,8, 10,

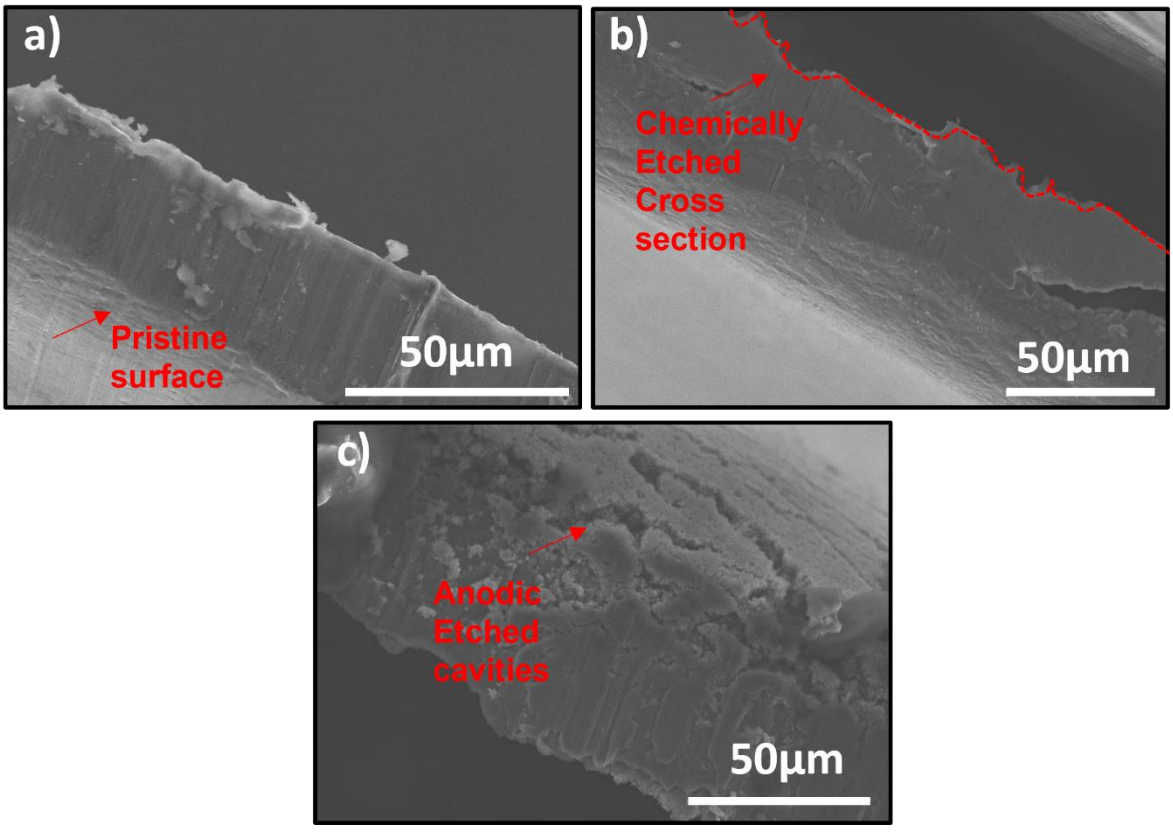

Figure 6.1 SEM images of the cross-sectional view of a) Al-30p b)Al-30CE c)Al-70

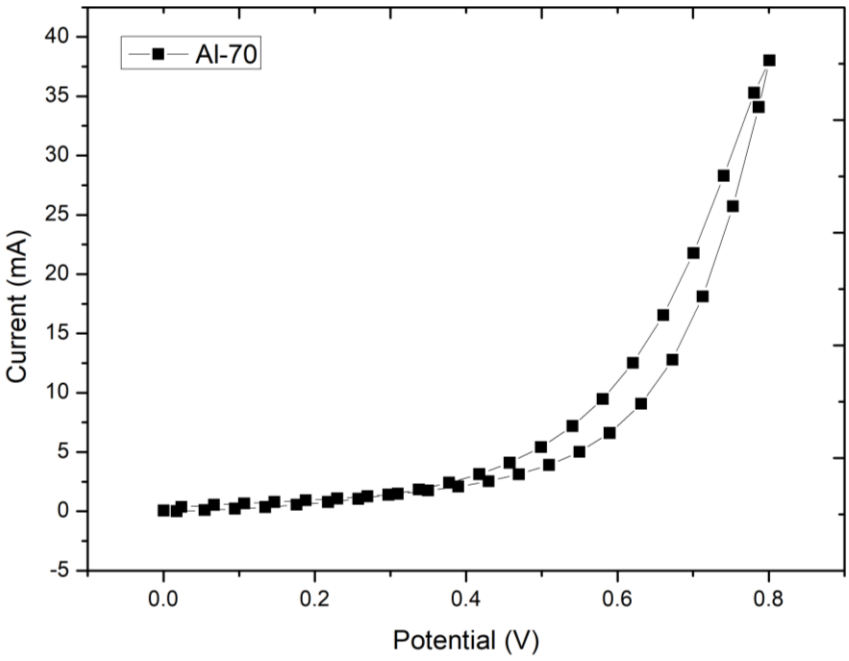

Figure 6.2 CV curve of Al-70 for the potential window of 0 to 0.8V